Aus der

Universitätsklinik für Thorax-, Herz- und Gefäßchirurgie Tübingen

Comparison of aortic remodelling after conservative treatment or thoracic endovascular repair in type B dissections

Inaugural-Dissertation
Zur Erlangung des Doktorgrades
der Medizin

der Medizinischen Fakultät
Der Eberhard Karls Universität
zu Tübingen

vorgelegt von

Andic, Mateja

2023

Dekan: Professor Dr. B. Pichler

1. Berichtersteller: Professor Dr. C. Schlensak
2. Berichtersteller: Professor Dr. G. Grözinger

Tag der Disputation: 21.11.2023

Table of Contents

1.Introduction……..….1

1.1. Anatomy of the aorta…….……..….1

1.2. The pathogenesis of aortic dissections…….…….3

1.2.1. Temporal classification……4

1.2.2. Anatomic classification……5

1.3. Impact of the dissection type on the management…….…….6

1.4. Clinical presentation……..….7

1.4.1. Pain……7

1.4.2. Blood pressure……...8

1.4.3. Neurologic symptoms…….……8

1.4.4. Organ malperfusion…….……8

1.5. Diagnostic evaluation……..9

1.5.1. Electrocardiography……....9

1.5.2. Echocardiography……9

1.5.3. Computed tomographic angiography…….……..10

1.5.4. Magnet resonance imaging……..…12

1.6. Treatment algorithm of the TBAD……..12

1.6.1. Medical treatment of TBAD……..12

1.6.2. Open surgical treatment of TBAD……..13

1.6.3. Endovascular treatment……....14

1.6.4. Anatomical prerequirements of TEVAR procedure……15

1.6.5. TEVAR related complications…….……16

1.7. The aim of the study……..17

2.Materials and methods……..……..…18

2.1. Study population……....18

2.2. Thoracic endovascular aortic repair procedure…….19

2.3. Diameter measurements…….20

2.4. Length measurements…….22

2.5. Baseline risk factors and their association with aortic enlargement…….23

2.6. Statistical analysis…….24

3.Results……..25

3.1. Cohort characteristics……..25

3.2. Procedural data and the follow-up……..….28

3.3. Aortic diameter growth rates……..29

3.4. Aortic length growth rates……...36

4.Discussion……40

4.1. Remodelling of aortic dissections…….…40

4.2. Conversion from conservative therapy to thoracic endovascular aortic repair…….…42

4.3. Aortic elongation……....43

5.Conclusions……46

6.Summary……...48

6.1. Summary (English version)……48

6.2. Summary (German version)……...49

7.Publication……52

8.References……...53

Autor Contribution……62

Acknowledgments……..……..63

Figures

Figure 1: The structure of the aortic wall……..…..**2**

Figure 2A: Three-dimensional (3D) reconstruction of the thoracic aorta…….....**3**

Figure 2B: Three-dimensional (3D) reconstruction of the abdominal aorta…….**3**

Figure 3A: Sagittal view of CTA of the type A aortic dissection……**7**

Figure 3B: Sagittal view of CTA of the type B aortic dissection……..…**7**

Figure 3C: 3D reconstruction of the TBD……..**7**

Figure 4A: 3D reconstruction of CTA showing distal stent induced new entry (d-SINE) after TBAD TEVAR treatment……**11**

Figure 4B: Sagittal view of CTA showing distal stent induced new entry (d-SINE) after TBAD TEVAR treatment……**11**

Figure 4C: Sagittal view of CTA showing the persistent dissection of the aortic root after ascending replacement in TAAD……..…**11**

Figure 5: 3D-reconstruction of the aorta with diameter landmarks……...**22**

Tables

Table 1A: Temporal Aortic Dissection classification……**4**

Table 1B: Anatomical Aortic Dissection classification…….**5**

Table 2: Signs of aortic remodeling……..**15**

Table 3: Baseline patients and dissection characteristics……...**26**

Table 4: Anatomic risk factors for aortic enlargement……...…**27**

Table 5: Periprocedural data……**29**

Table 6: Axial aortic diameter growth rate (mm/year) in dissections after conservative therapy and TEVAR in the acute phase……...**32**

Table 7: Axial aortic diameter growth rate (mm/year) in non-converted and converted chronic dissections before conversion to TEVAR……....**33**

Table 8: Anatomic risk factors for aortic enlargement in the non-converted and converted chronic dissection subgroup……....**34**

Table 9: Axial aortic growth rate (mm/year) in chronic dissection before and after conversion to TEVAR……..…**35**

Table 10: Longitudinal aortic growth rate (mm/year) in dissections after conservative therapy and TEVAR in the acute phase……...**37**

Table 11: Longitudinal aortic growth rate (mm/year) in non-converted and converted chronic dissections before conversion to TEVAR……....**38**

Table 12: Longitudinal aortic growth rate (mm/year) in chronic dissection before and after conversion to TEVAR……**39**

Abbreviations

BCT	brachiocephalic trunk
CeT	celiac trunk
CSFD	cerebrospinal fluid drain
CT	computed tomography
CTA	computed tomographic angiography
d-SINE	distal stent induced new entry
dP/dT	the force of left ventricular ejection
ECG	electrocardiography
EIA	extern iliac artery
EVAR	endovascular aortic repair
FL	false lumen
HA	hypogastric artery
IMA	inferior mesenteric artery
IVUS	intravascular ultrasound
LCCA	left carotid artery
LRA	left renal artery
LSA	left subclavian artery
MAP	mean arterial pressure
MRI	magnetic resonance imaging
OR	open repair
PTFE	polytetrafluoroethylene
RRA	right renal artery
SCI	spinal cord ischemia
SMA	superior mesenteric artery
TAAD	type A aortic dissection
TBAD	type B aortic dissection
TEE	transesophageal echocardiography
TEVAR	thoracic endovascular aortic repair
TL	true lumen
TTE	transthoracic echocardiography

1 Introduction

1.1 Anatomy of the aorta

The aorta is the greatest vessel in the human body and through its branches, it serves as a blood provider to the organs and the extremities. Microscopically, the aortic wall consists of three main layers. The intima layer comprises the endothelium and the internal elastic lamina, thus, it interacts directly and continuously with the blood components and prevents atherosclerotic and thrombotic lesions on the inner aortic wall surface. 80% of the aortic wall consists of a media layer. It ensures the integrity of the aortic wall with pronounced elasticity provided by the high concentration of elastic and collagen fibers and the smooth muscle cells found in this layer (Silver et al., 2001). The adventitia is the most extern aortic wall collagenous layer, whose primary function is the blood perfusion of the aortic wall through vasa vasorum (Figure 1).

Macroscopically, the aorta extends from the aortic valve to the aortic bifurcation in the abdomen, and, thus, it is subdivided into the thoracic aorta above the diaphragm and the abdominal aorta located below the diaphragm. The thoracic aorta consists of three anatomical entities. First, the ascending aorta from the aortic valve to the origin of the brachiocephalic trunk (BCT) with the coronary arteries (right main coronary artery and right coronary artery) being the only branches originating from the ascending portion. Second, the aortic arch, which accommodates the brain and upper extremities vessel origins: BCT, left carotid artery (LCCA) and the left subclavian artery (LSA), and, third, the descending aorta, which extends from the LSA to the diaphragm incorporating the origins of the bronchial arteries (vasa privata of the lung) and intercostal artery pairs III-XII (Figure 2). The latter are involved in the spinal collateral network circulation and their extensive sacrifice during open or endovascular aortic procedures may provoke spinal ischemia (Etz et al., 2008a, Etz et al., 2008b, Etz et al., 2008c).

The abdominal aortic portion comprises the origins of the reno-visceral arteries, namely those of the celiac trunk (CeT), the superior mesenteric artery (SMA), the right (RRA) and left renal artery (LRA), and the inferior mesenteric artery (IMA).

Pairwise emerging lumbar arteries contribute to the perfusion of the lumbosacral musculature and, thus, to the spinal collateral network. At the level of the lumbar vertebra 4, the infrarenal aorta divides into the commune iliac arteries, which distribute the blood flow to the pelvis (hypogastric artery; HA) and the lower extremity (extern iliac artery; EIA).

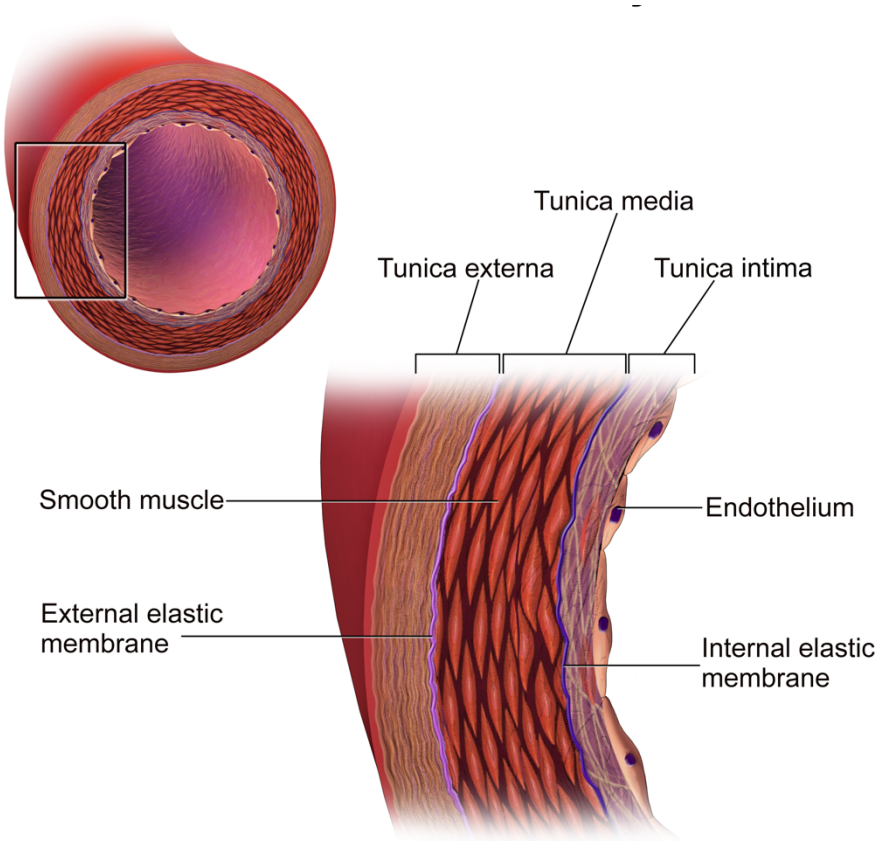

Fig. 1:

The structure of the aortic wall. (Blausen.com staff (2014). “Medical gallery of Blausen Medical 2014”. Wikijournal of Medicine 1 (2).

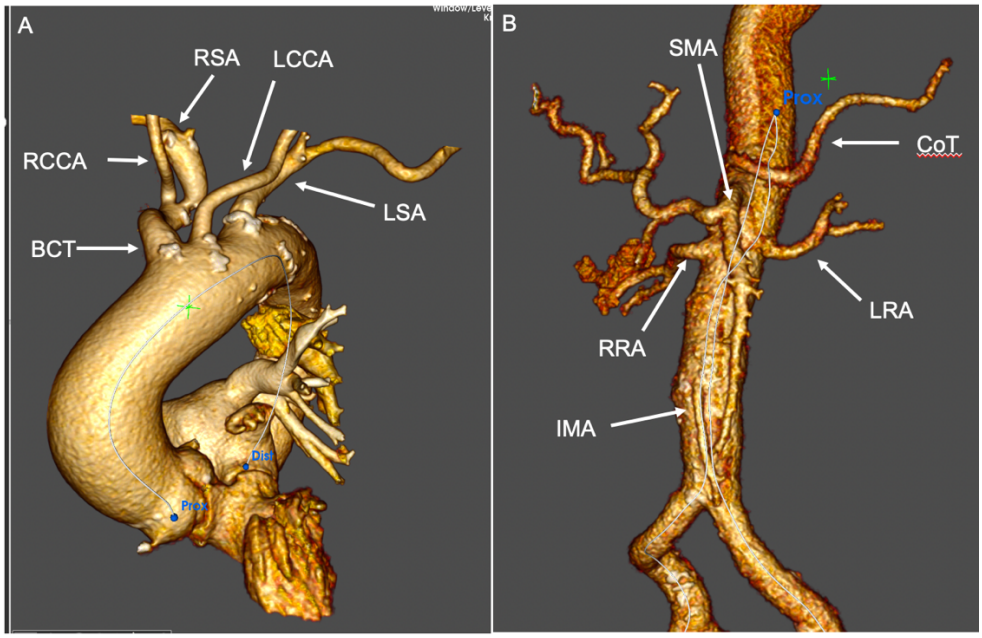

Fig. 2:

Three-dimensional (3D) reconstruction of the: A - thoracic aorta and major branches: brachiocephalic trunk (BCT), right carotid artery (RCCA), right subclavian artery (RSA), left carotid artery (LCCA), left subclavian artery (LSA); B – abdominal aorta and major branches: celiac trunk (CoT), superior mesenteric artery (SMA), right renal artery (RRA), left renal artery (LRA), inferior mesenteric artery (IMA).

1.2 The pathogenesis of aortic dissections

The aortic wall structure ensures its high elasticity and responsiveness to the shear stress and blood pressure changes during the cardiac cycle. However, hypertension, connective tissue diseases, and pre-existing intima lesions (e. g. penetrating aortic ulcers) may lead acutely to the longitudinal separation of the aortic layers: the aortic dissection. From the site of the proximal entry tear, the intimo-medial layer is cleaved both circumferentially and longitudinally (Khan and Nair, 2002) which leads to the development of the biluminal dissection architecture with the true lumen (TL) limited by the intima, as well as, the false

lumen (FL) surrounded by the aortic wall layers. Thus, the dissection flap (or dissection membrane) divides the TL and the FL. Distal connections between FL and TL lumen are called re-entries and constitute dissection membrane perforations, mostly found at the level of aortic branch origins. FL perfusion and pressurization of the weakened aortic wall may cause early or late aortic dilatation or compression of the TL (true lumen collapse), which may lead to aortic rupture and downstream organ malperfusion, respectively.
Aortic dissections are classified according to the time since dissection onset and the anatomical extent (Table 1).

1.2.1 Temporal classification:

Acute, subacute, and chronic aortic dissections are being differentiated. In the first 2 weeks after symptoms onset, the dissection is regarded as an acute dissection. After 2 weeks the dissection is being referred to as subacute dissection and after 90 days as chronic dissection (Table 1A).

TABLE 1A Temporal Aortic Dissection classification

Temporal classification	
Acute	≤14 days
Subacute	15-90 days
Chronic	>90 days

TABLE 1B Anatomical Aortic Dissection classification

Anatomical classification				
DeBakey	Typ I	Typ II	Typ III	
Stanford	Typ A		Typ B	
			Uncomplicated	Complicated by the presence of
				Rapid aortic expansion
				Aortic rupture
				Shock
				Ischaemia (visceral, renal, limb)
				Paraplegia/paresis
				Peri-aortic haematoma
				Recurrent or refractory pain
				Refractory hypertension

1.2.2 Anatomic classification:

The DeBakey classification includes both the entry localization and the extent of the aortic dissection and differentiates four types: Type I: Dissection originates from the ascending aorta and extends into the descending aorta; type II: Dissection is limited to the ascending aorta; type IIIa: dissection is limited to the descending aorta and type IIIb: dissection includes the descending aorta and the abdominal aorta (Debakey et al., 1965).

The Stanford classification is based on the localization of the proximal entry tear (Table 1B). The Stanford type A dissection (TAAD) involves the ascending aorta, and the Stanford type B (TBAD) extent is only limited to the descending aorta (Figure 3).

1.3 Impact of the dissection type on the management

In Europe, the Stanford classification is widespread and used to direct the initial therapy. Untreated TAAD is associated with a high risk of lethal complications. Therefore, the first-line therapy is the elimination of the proximal entry tear by dacron graft replacement of the ascending aorta to prevent complications, which include aortic rupture, cardiac tamponade, myocardial infarction, or severe aortic valve regurgitation. Those complications are in 25% of patients associated with hypotension (systolic blood pressure <90mmHg). Open repair methods in TAAD include supracoronary ascending aorta replacement, aortic root replacement, proximal hemiarch and total arch replacement (Evangelista et al., 2018).
Acute TBAD may present with symptoms and signs which define a complicated TBAD (Table 1B). The mortality in patients with complicated TBAD is significantly higher compared with non-complicated TBAD (20,0% vs. 6,1%) (Trimarchi et al., 2012). Thoracic endovascular aortic repair (TEVAR) has shown more favorable outcomes in terms of in-hospital mortality, compared to open repair (OR), leading TEVAR to be the first-line therapy in complicated TBAD (Zeeshan et al., 2010). The aim of the therapy is to reestablish the perfusion of affected organs and to prevent the further expansion of false lumen (FL) (Riambau et al., 2017). Almost 50% of patients with TBAD present without complications (Riambau et al., 2017). Initial therapy in all TBAD is a medical treatment with antihypertensive agents, to reduce aortic wall stress through high blood pressure (BP) (Sakakura et al., 2007).

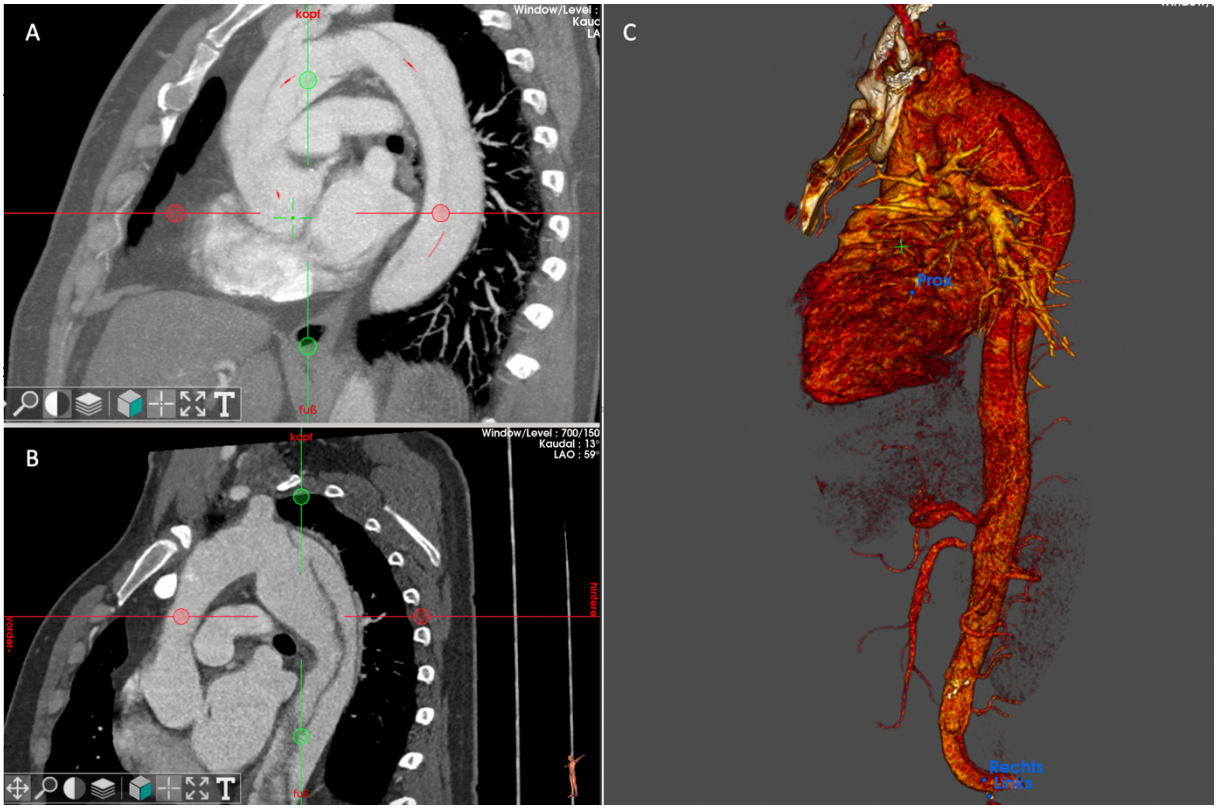

Fig. 3:

A – Sagittal view of CTA of the type A aortic dissection (TAAD); B – sagittal view of CTA of the type B aortic dissection (TBAD); C – 3D reconstruction of the TBD.

1.4 Clinical presentation

1.4.1 Pain

The most common presenting symptom, reported in more than 93% of patients with aortic dissection is severe tearing interscapular pain. An abrupt onset is presented in 85% of patients. In TAAD typical symptom is anterior chest pain. Abdominal and back pain is frequently found in patients with TBAD (Hagan et al., 2000).

The pain has been localized in the back in 46% of patients with TAAD and 64% of patients with TBAD, whereas the abdominal pain was present in up to 21% of the patients with TAAD and 43% of the patients with TBAD (Hagan et al., 2000).

1.4.2 Blood pressure

The presence of hypertension was detected in 70% of patients with acute TBAD in comparison with 36% in patients with TAAD on initial clinical examination (Hagan et al., 2000).
Hypotension was noted in 11% of patients with TAAD, which may be an early sign of cardiac tamponade or aortic valve insufficiency. Initial systolic blood pressure below 100mmHg was rare in the group of patients with TBAD (2%). Pulse deficit was more often seen in patients with TAAD (19% vs. 9%) (Hagan et al., 2000).

1.4.3 Neurologic symptoms

Syncope was more common in patients with TAAD than TBAD and occurred in 19% of patients (Nallamothu et al., 2002). The syncope is often a result of cardiac tamponade or dissection expansion in the brachiocephalic vessels (Nallamothu et al., 2001). Similarly, a stroke was more presented in the group of patients with TAAD (6% vs. 2%) (Hagan et al., 2000).
Spinal cord ischemia was more often detected in patients with TBAD, due to interruption of intercostal vessel blood flow (Syed and Fiad, 2002).
Paresthesia, Horner´s syndrome (compression of sympathetic ganglion), or harshness of voice (compression of the recurrent laryngeal nerve) as a result of direct compression of peripheral nerves were rare (Khan et al., 1999) (Lefebvre et al., 1995).

1.4.4 Organ malperfusion

Malperfusion syndrome is a result of end-organ ischemia secondary to aortic branch compromise due to the dissection process. It may include nearly all major vascular beds (Crawford et al., 2016).

Organ malperfusion symptoms depend on the obstruction of affected vessels, although the signs and symptoms of critical ischemia may be absent in the presence of collateral circulation (Cambria et al., 1988).

The obstruction of affected aortic branches can be dynamic or static. The more common mechanism is dynamic obstruction, occurring in 80% of malperfusion syndromes (Williams et al., 1997b). The vessel ostium remains anatomically intact, but volume flow is compromised through the compressed true lumen or the prolapse of the dissection flap into the ostium (Williams et al., 1997b).

In static obstruction the dissection extends into the aortic branch wall, leading directly to obstruction or occlusion (Williams et al., 1997b). In addition, thrombus formation beyond the compromised origin may further deteriorate the perfusion (Williams et al., 1997a).

The first symptom of malperfusion syndrome is typically abrupted pain, whose localization depends on compromised aortic branch vessels (Hagan et al., 2000). Apart from the pain, malperfusion syndrome presents through neurologic deficit, pulse differential, and dysfunction of an affected organ system. In the case of supra-aortic vessel involvement, the first signs may include pulse deficit in the upper extremities, a side difference in blood pressure measurements, stroke, as well as deterioration in mental status. The affection of mesenteric vessels may lead to mesenteric ischemia with abdominal pain, metabolic acidosis, and rising lactate. Lumbar pain, elevated creatinine, potassium and lactate-dehydrogenase levels may be detected in the case of renal artery involvement (Crawford et al., 2016).

1.5 Diagnostic evaluation

1.5.1 Electrocardiography (ECG)

The ECG changes are not dissection-specific. ST segment depression and T-wave abnormalities are the most common changes found in aortic dissections and may be signs of a pericardial effusion or a cardiogenic shock (Hirata et al.,

2010). ST-segment elevation was reported in 8.2% of patients with TAAD (Hirata et al., 2010).

1.5.2 Echocardiography

Although the sensitivity and specificity of transthoracic echocardiography (TTE) have been improved in the diagnostic evaluation of aortic dissections, transesophageal echocardiography (TEE) is still the ultrasound method with the highest sensitivity/specificity (Evangelista et al., 2010).

TEE surpasses the technical limitations of the TTE, such as narrow intercostal spaces, emphysema, and false-positive results due to artifacts (Granato et al., 1985, Adachi et al., 1991).

TEE may detect entry tear sites, FL status, pericardial or pleural effusions, and involvement of coronary arteries (Erbel, 1993). Color Doppler may be used to show the difference between flow velocities in TL and FL (Erbel, 1993).

The limitation of the TEE is found in the imaging of the proximal aortic arch and the aorta below the diaphragm (Erbel et al., 1990).

1.5.3 Computed tomographic angiography

Computed tomographic angiography (CTA) is considered to be the gold standard method in the diagnosis of aortic dissections (Hagan et al., 2000).

CTA allows for precise aortic imaging and proximal entry tear sites, making a good base for planning an open and particularly endovascular intervention. Mostly, following an undissected segment of the aorta from proximal to distal, it is possible to differentiate FL from TL (LePage et al., 2001). Although, this may not be possible in the circumferential dissection of the aortic root. In more than 90% of cases, the TL is narrower than the FL in the descending thoracic aorta, which may facilitate differentiation. Moreover, intraluminal partial or complete thrombosis may also be used as an indicator of the false lumen (LePage et al., 2001).

Diagnosis of malperfusion syndromes may be based on CTA imaging and confirmed by symptoms or physiological and biochemical abnormalities (Crawford et al., 2016). In the case of dynamic malperfusion the additional evaluation of the dissection membrane with intravascular ultrasound (IVUS) may be used to additionally assess the membrane behavior (Grewal et al., 2021).
Planning of the endovascular procedure is performed with a CTA dataset and 3D multiplanar and centerline reformats with dedicated software.
In the follow-up, CTA allows for exact diameter measurements to determine false lumen expansion (post-dissection aneurysm formation) or to assess the therapy success or complications that may arise from the endovascular endograft or open repair (Figure 4).

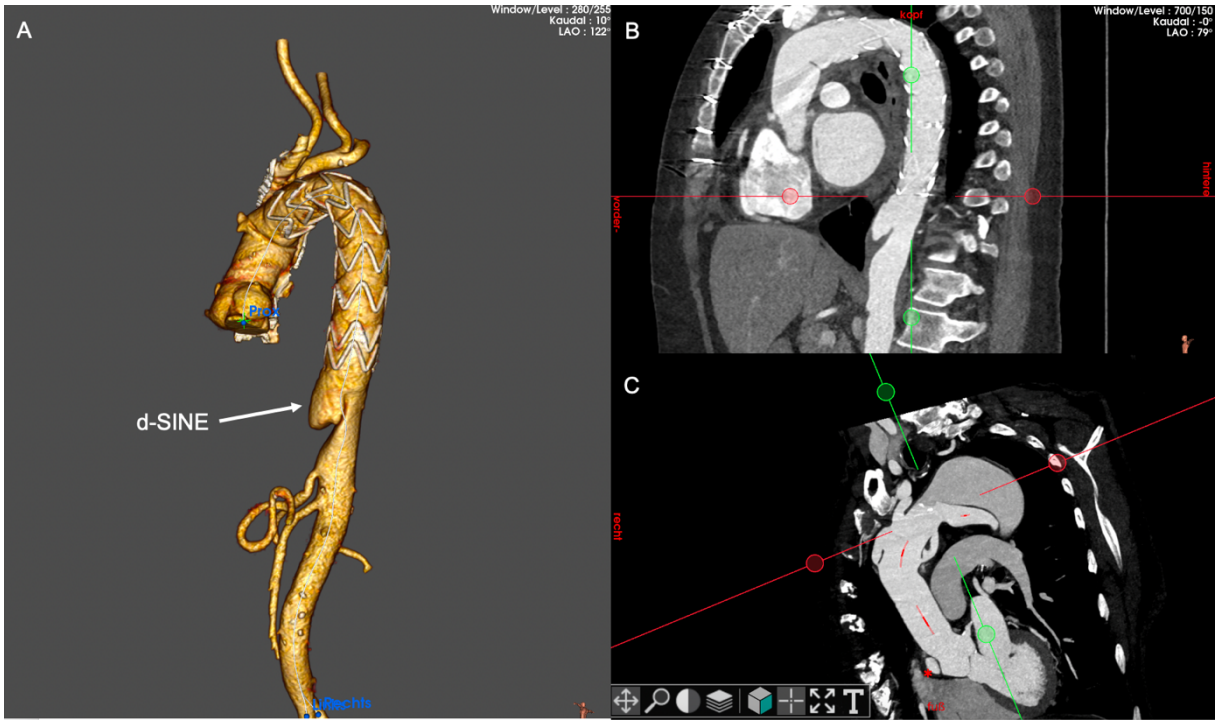

Fig. 4:
A – 3D reconstruction and B – sagittal view of CTA showing distal stent induced new entry (d-SINE) after TBAD TEVAR treatment; C – sagittal view of CTA showing the persistent dissection of the aortic root after ascending replacement in TAAD (*).

1.5.4 Magnetic resonance imaging

Magnetic resonance imaging (MRI) is a highly sophisticated method for the diagnosis of aortic dissection, with a sensitivity of 95% to 98% and a specificity of 94% to 98% (Moore et al., 2002, Fruehwald et al., 1989, Tomiguchi et al., 1994, Shiga et al., 2006). MRI does not require ionizing radiation and ensures the accurate detection of the site of the proximal entry tear and the differentiation between false and true lumen, as well as the involvement of aortic branches in the dissection process (Prince et al., 1996).

The limitations of the MRI are long examination times and a shortage of immediate availability. In addition, MRI is contraindicated in patients with metallic implants, like cardiac pacemakers or defibrillators (Baliga et al., 2014). Therefore, MRI may be used during the follow-up in selected patients to assess the status of the dissected aorta and to reduce the radiation exposure, while the use in acute setting is not practicable.

1.6 Treatment algorithm of the TBAD

1.6.1 Medical treatment of TBAD

The initial therapy for all patients with the diagnosis of TBAD is the reduction of systolic blood pressure to 100-120 mmHg, to prevent further expansion of aortic dissection and rupture (Isselbacher, 2005).

In case of suspected aortic dissection, intravenous application of antihypertensive therapy should be started, except in patients with hypotension (Isselbacher, 2005).

While TAAD and complicated TBAD require an open or endovascular surgical procedure after initial medical management, respectively, uncomplicated TBAD remains treated conservatively.

An intravenous beta blocker, such as metoprolol, propranolol, labetalol, esmolol, and atenolol is infused in the acute phase until the evidence of effective beta-blockade, reducing heart rate is achieved (Suzuki et al., 2012). Beta-blockers

were shown to reduce aortic wall shear stress and may influence the early and late outcomes after aortic dissections (Allen et al., 2016). Calcium channel antagonists (verapamil, diltiazem) and renin-angiotensin inhibitors can be used in patients who do not tolerate or do not respond to beta blockers (Genoni et al., 2001). If not contraindicated, beta-blocker therapy is recommended to be initiated before the vasodilator to avoid an increase of dP/dT (the force of left ventricular ejection) through reflex sympathetic stimulation (Isselbacher, 2005).

Pain symptoms may reduce with the application of antihypertensive therapy or need to be treated with analgesics (Xiang et al., 2021).

During the acute period, the patients should be supervised in the intensive care unit with continuous blood pressure monitoring. After successful blood pressure and pain relief, intravenous therapy can be transitioned to oral antihypertensives (Isselbacher, 2005).

Patients with TBAD who remain treated medically should be monitored regularly with CT angiography (Isselbacher, 2005).

1.6.2 Open surgical treatment of TBAD

The aim of the open surgical repair is to replace the dissected part of the aorta with the dacron graft and to prevent further expansion and rupture (Riambau et al., 2017). The exposure of the descending aorta is gained via a left-sided postero-lateral thoracotomy through the fourth intercostal space. After preparation, the proximal and distal thoracic aorta is cross-clamped, and the descending part is opened longitudinally. The cranial extension of the dissection is identified, and the aorta is transected proximally. The dacron graft is sewn end to end with a 4-0 or 5-0 monofilament suture. After completing the proximal anastomosis, the distal aorta is transected, and the aortic graft is sewn again using a 4-0 monofilament suture. Left heart bypass is performed to preserve the perfusion of the vital organs and the lower limbs during clamping. The oxygenated blood from the left side of the circulation (left atrium, left ventricle, left pulmonary

vein) is shunted into the circulation below the distal clamping (left common femoral artery or left common iliac artery) (Nauta et al., 2016).
In the case of complicated TBAD, with the need for invasive treatment, endovascular treatment is preferred over open surgical repair due to a better survival rate of patients with endovascular therapy. The mortality rate associated with open repair has ranged from 6% to 69% in the treatment of acute TBAD (Coselli, 1994, Neya et al., 1992, Svensson et al., 1990, Trimarchi et al., 2006, Verdant et al., 1995).
The IRAD registry included 476 individuals with TBAD who were treated with open surgical repair. In-hospital mortality was observed in 29% (Trimarchi et al., 2006).

1.6.3 Endovascular treatment

The initial therapy for all patients with aortic TBAD should be medical regulation of systolic blood pressure and pain, to avoid fatal complications (Kaji, 2018).
Although patients with uncomplicated TBAD are primarily treated medically, more than three-quarters develop post-dissection aneurysms in the chronic dissection phase, requiring endovascular treatment (Schepens, 2018). Therefore, the selective early endovascular treatment of patients with uncomplicated TBADs, who are at risk of aneurysm development should be considered. The early risk factors include the diameter of the proximal entry tear >10 mm, the proximal entry tear localization in the lesser aortic curvature, FL diameter ≥22mm and initial aortic diameter ≥40 mm at dissection onset (Mustafi et al., 2020).

For complicated TBAD thoracic endovascular aortic repair (TEVAR) is the therapy of the first choice. The aim of this procedure is to induce false lumen thrombosis after the coverage of the proximal entry tear with an aortic endograft, which reduces the blood pressure in the false lumen, induces the expansion of the true lumen, and prevents aneurysm formation (Onitsuka et al., 2004). These morphological changes are described as aortic remodeling (Table 2.).

TABLE 2: Signs of aortic remodeling

Remodeling points
TL Expansion
FL Reduction
Maximal aortic diameter change
TL/FL Ratio
Total aortic volume
FL Thrombosis rate
TL/FL Volumetry
Stent graft remodeling /migration

1.6.4 Anatomical prerequirements of TEVAR procedure

Being a minimally invasive treatment, TEVAR highly depends on anatomical prerequirements of the aorta and iliofemoral arteries. An adequate proximal landing zone has shown to be the most important parameter for long-term success (AbuRahma et al., 2009). A healthy, non-dissected, and non-aneurysmal aortic segment with a length of 15-25 mm may be regarded as an appropriate landing zone for TEVAR (Czerny et al., 2010). The landing zone diameter size can extend from 16 to 42 mm, given that the available stent grafts are oversized and vary from 21 to 46 mm. The recommended oversizing is 15-20% and 0-10% for an aortic aneurysm or aortic dissection, respectively (Liu et al., 2016).

The most used classification today is Ishimaru`s scheme defining the five TEVAR proximal landing zones.

Zone 0 includes the ascending aorta and the origin of the brachiocephalic artery. Zone 1 includes the origin of the left common carotid artery. Zone 2 includes the

origin of the left subclavian artery. Zone 3 includes the proximal descending aorta distal from the left subclavian artery and down to the T4 vertebral body. Zone 4 includes the remainder of the thoracic aorta (Lin et al., 2013).
The aortic arch angulation must be considered, as severely angulated aortas may require more oversizing for appropriate apposition. There is no clear consensus about the calcification in the proximal landing zone. Dubois et al. categorized the distal landing zone as compromised in aortas with >25% circumferential mural calcification and >50% cross-sectional thrombus (DuBois et al., 2021).

1.6.5 TEVAR related complications

One of the most severe and potentially lethal outcomes is a retrograde TAAD, whose risk increases with the use of the proximal bare spring stent grafts and proximal balloon dilatation (Eggebrecht et al., 2009).
Spinal cord ischemia (SCI) is associated with postoperative hypotension (MAP<65 mmHg), low hemoglobin level (<120 g/L in females, <110 g/L in the male), the extent of the aortic coverage and preoperative renal insufficiency (Schlosser et al., 2009, Xue et al., 2018). The placement of cerebrospinal fluid drain (CSFD) prior to TEVAR reduces the risk of SCI from 10-20% to 2,3-10% (Epstein, 2018).
Stroke develops in 3-10% of TEVAR patients and is related to prolonged manipulation of catheters and wires in the aortic arch (Buth et al., 2007).
Covering the origin of the left subclavian artery (LSA) may be associated with higher SCI, stroke and arm ischemia risks (Xie et al., 2021). Thus, subclavian artery revascularization may reduce the risk of these complications, preserving the blood flow through the left vertebral artery and the LSA (Bartos et al., 2020).

1.7 The aim of the study

Which factors and events lead both to further progression of dissection and to complications remains the subject of discussion. The purpose of the research is to detect the risk factors that precede conversion, which can help to identify uncomplicated TBADs that might benefit from TEVAR in early phases.
Furthermore, the goal of the study was to assess aortic remodelling after acute TEVAR and in conservatively treated patients, the assessment of the conversion rate to TEVAR, and the impact of the TEVAR on the remodeling of converted patients (Mustafi et al., 2020).

2 Materials and methods

2.1 Study population

Between 2011 and 2017 all patients with TBAD were retrospectively obtained from medical records of the University Hospital Tübingen Germany. Aortic dissection was classified as TBAD according to the Stanford classification. All patients enrolled in the study acquired at least one baseline computer tomography (CT) scan and an additional CT after a minimum follow-up of 6 months (Mustafi et al., 2020).

The study population was divided into two groups, according to their therapeutic regimen. Group A included the patients with uncomplicated TBAD who were treated conservatively, while group B included the patients with complicated TBAD who were treated with TEVAR in the acute phase. Complicated acute TBAD was defined by the presence of at least one of the following changes: malperfusion syndrome, resistant and refractory hypertension and pain, periaortic hematoma, aortic rupture, and diameter enhancement within 48 h after onset of symptoms (Mustafi et al., 2020).

Group A was divided into two subgroups. The “non-converted” subgroup was composed of patients with uncomplicated TBAD who remained treated conservatively. The patients who developed complications in the “follow-up” period and therefore required TEVAR procedure were aligned in the “converted” subgroup (Mustafi et al., 2020).

The indications for conversion from conservative to endovascular treatment were the expansion of total aortic diameter to ≥55 mm or diameter progress of ≥5 mm/year in CT scans performed during the follow-up (Mustafi et al., 2020).

CT studies were obtained at University Hospital Tübingen using a second-generation dual-source CT scanner (Somatom Definition Flash; Siemens Healthcare, Erlangen, Germany).

All CT scans were recorded in the arterial phase, 35-40 sec after intravenous radiocontrast administration, and had a minimum slice thickness of 3 mm.

The characteristic of the observed population included age, gender, and time between the index event and the TEVAR procedure.

As the analyzed data were collected retrospectively for research purposes, written consent from the patients for this study was not necessary.
The study was approved by our center´s local ethic committee (306/2019BO2) (Mustafi et al., 2020).

2.2 Thoracic endovascular aortic repair procedure

The thoracic endovascular aortic repair (TEVAR) procedure was performed under general anesthesia. The patients were placed in the supine position. To prevent SCI, a CSFD was placed one day before the operation in all elective patients.
In the case of covering the origin of the left subclavian artery with TEVAR, the left carotid-axillary bypass was placed before deployment (Bartos et al., 2020).
For carotid-axillary bypass, access to the left carotid commune artery was gained by a longitudinal incision along the anterior border of the sternocleidomastoid muscle (Bartos et al., 2020). The left axillary artery was exposed through an infraclavicular incision parallel to the clavicle and by splitting the fibers of the pectoralis major muscle and medial traction of the pectoralis minor muscle (Bartos et al., 2020). The tunneling was accomplished from both sides with blunt dissection with fingers behind the internal jugular vein and immediately under the clavicle. A 6mm ringless polytetrafluoroethylene (PTFE) graft (GORE-TEX vascular graft, W.L. Gore and Associates, Flagstaff, AZ, U.S.A.) was tunneled and heparin was given intravenously (100 I.U./kg BW). The carotid shunting was not used for this procedure. The anastomoses were made using a 6-0 Prolene suture. After the procedure, good pulses were established (Bartos et al., 2020).
The access site for the TEVAR implantation was the femoral artery. On the device access site, a femoral cut-down was performed and an 11-French (Fr) sheath was placed into the common femoral artery. An angled catheter and guidewire were used to access the abdominal aorta, and then the ascending aorta under fluoroscopic guidance. The guidewire was then exchanged for the double-curved Lunderquist extra-stiff wire (Cook Medical, Bloomington, IN, USA) which was

placed to the aortic root. A percutaneous 6 Fr sheath was placed in the contralateral femoral artery and a pigtail angiography catheter was positioned in the ascending aorta (Bartos et al., 2020, Mustafi et al., 2020).

The diameter of the proximal and distal neck and the length had been measured using the preoperative CT scan and based on those measurements the corresponding stent graft had been chosen. The pigtail catheter was used to perform an aortogram of the area of interest. Before device deployment, the respiratory device was paused, and the procedure continued under rapid pacing. A repeated angiogram was performed multiple times to confirm the positioning of the device. After correct graft positioning, all the wires and catheters were removed, and the femoral artery was repaired in a standard way. After the procedure, the distal pulses were checked and well established (Bartos et al., 2020, Mustafi et al., 2020).

2.3 Diameter measurements

CTA datasets were performed with the OSIRIX-MD (PIXMEO, Bernex, Switzerland) PACS Viewer and image-processing software package. The aorta was visualized using curved multiplanar reformats. The same anatomic landmarks were used at all CT scans (baseline and follow-up scans). The reconstruction was made from the aortic valve to 1 cm below the aortic bifurcation. All diameters were measured by manually defining the aortic central line with a 3D-Bezier-curve in the transversal, coronal, and longitudinal CTA reconstructions (Kruger et al., 2017). The true and false lumen, and the thrombus, if present, were included in reconstruction and measuring.

The aorta is commonly divided into five main anatomic segments: the aortic root, the tubular portion of the ascending aorta, the aortic arch, the descending aorta, and the abdominal aorta (Goldstein et al., 2015).

In our study, the landmarks were defined by international guidelines with slight modifications (Goldstein et al., 2015). Due to reproduction complexity, the

diaphragm as a landmark was replaced by the orifice of the coeliac trunk (Lescan et al., 2017).

The pencil tool was used to delineate the outer-to-outer aortic diameter at defined landmarks. To minimize errors due to non-circulatory shaped aortas in the short axis, the optimized aortic diameter was calculated according to the following formula: $d = c/\pi$ [(d=diameter (mm); c=circumference (mm)] (Mustafi et al., 2020).

For the evaluation of the aortic diameters, the following landmarks were applied (Mustafi et al., 2020): (Figure 5):

(D1) mid-ascending aorta (halfway between sinotubular junction and the proximal orifice of the brachiocephalic trunk)

(D2) proximal orifice of the brachiocephalic trunk

(D3) mid-arch (halfway between the proximal orifice of the brachiocephalic trunk and distal left subclavian artery orifice)

(D4) proximal descending aorta (directly downstream of the left subclavian artery)

(D5) mid-descending aorta (at the level of the pulmonary artery bifurcation)

(D6) thoracoabdominal (proximal orifice of the coeliac trunk)

(D7) mid-abdominal (halfway between the proximal orifice of the coeliac trunk and aortic bifurcation).

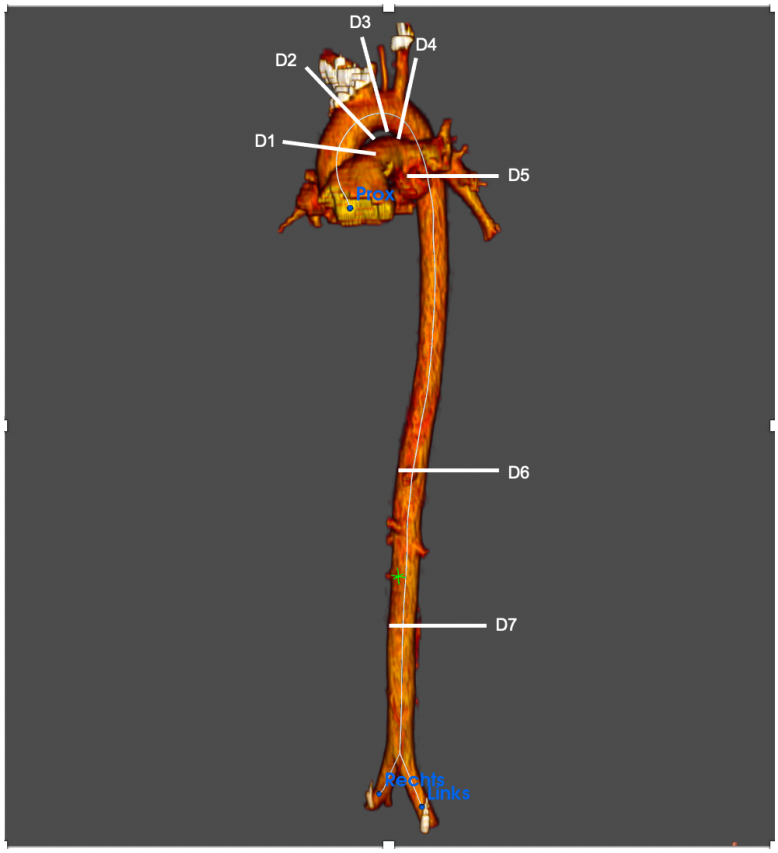

Fig. 5:
3D-reconstruction of the aorta with diameter landmarks D1-D7. D1: mid-ascending aorta; D2: proximal orifice of the brachiocephalic trunk; D3: mid-arch diameter; D4: proximal descending aorta; D5: mid-descending aorta; D6: distal descending diameter at the coeliac trunk; D7: mid-abdominal diameter.

2.4 Length measurements

After the determination of diameter landmarks (D1-D7), the length parameters (L1-L4) were measured. The aortic segments for length measurements were defined by international guidelines and determined as follows (Goldstein et al., 2015):
(L1) ascending aorta (sinotubular junction – proximal orifice of the brachiocephalic trunk)

(L2) aortic arch (proximal orifice of the brachiocephalic trunk – distal orifice of the left subclavian artery)
(L3) descending aorta (distal orifice of the left subclavian artery– proximal orifice of the coeliac trunk)
(L4) abdominal aorta (proximal orifice of the coeliac trunk – aortic bifurcation)

2.5 Baseline risk factors and their association with aortic enlargement

The baseline risk factors that predicted the aortic enlargement were evaluated in the initial CT scans. The measurements included proximal entry diameter >10 mm, baseline aortic diameter >40 mm, and baseline false lumen diameter >22 mm.
The mean proximal entry diameters were measured in curved multiplanar reformat according to the formula $d = (a + b)/2$, where (a) stands for diameter measurement in the long axis and (b) for diameter measurement in short axis (Mustafi et al., 2020).
The baseline aortic diameter and baseline false lumen diameter were measured, as explained previously, using a pencil tool and calculated according to the following formula: $d = c/\pi$ [(d=diameter (mm); c=circumference (mm)].
Anatomic factors such as proximal entry at the smaller aortic arch curvature and partial false lumen thrombosis were also included in the analysis (Mustafi et al., 2020).

2.6 Statistical analysis

JMP 14 software (SAS, Cary, NC, USA) was used for the statistical analysis. Categorical data were presented as absolute numbers with percentages. Continuous data were shown as mean +/- standard deviation. Leven´s test was used to determine the equality of variances and the Shapiro-Wilk test for normality. Categorical data were tested with Fisher´s exact test. The unpaired or paired t-test was used to compare normal distributed variables. Nonparametric data were analyzed with Wilcoxon signed rank test and Mann-Whitney U-test. The association between diameter growth and length growth changes was analyzed with correlation analysis. Spearman Rho test was used to investigate a correlation between length and diameter measurements. P-values <0.05 were considered statistically significant (Mustafi et al., 2020).

3 Results

3.1 Cohort characteristics

The study included 74 patients with TBAD between 2011 and 2017. They were divided into two groups. Group A consisted of 50 patients with uncomplicated TBAD, who were treated conservatively (n=32) or converted to TEVAR (n=18). In the follow-up period. In group B were 24 patients with complicated TBAD, treated with TEVAR in the acute phase. The demographic, perioperative, and follow-up data are provided in Table 3.

The mean follow-up time was 1625±209 days for group A and 554±129 days for group B. No patient was lost to follow-up. In both groups, the mean age was 62 years (group A ±2; group B ±5; P=0.99, Table 3). In total, the prevalence of the female gender was lower compared to the male gender (A: 23%, B: 5%; P=0.17, Table 3) (Mustafi et al., 2020).

In group B the patients were treated with TEVAR after 4±1 days. Of 50 patients in group A, 36% (n=18) had to be converted from conservative therapy to TEVAR after the follow-up period of 1298±355 days (Table 3). The indications for conversion were total aortic diameter ≥55 mm, which was present in 18% (n=9) of patients in group A, and progress of the aortic diameter ≥5 mm/year, presented in 18% (n=9) of patients (Mustafi et al., 2020).

Anatomic risk factors for aortic enlargement were equally distributed in both groups, with the prevalence of entry at the smaller aortic arch curvature at 11% (n=8) in group A and 12% (n=9) in group B and partial true lumen thrombosis at 20% (n=15) in the group A and 15% (n=11) in the group B (Table 4). The baseline aortic diameter was >40 mm in 58% of all patients (A: 42%, B: 16%; P=0.45, Table 4).

The baseline false lumen diameter >22 mm was less present in a group of patients with complicated acute TBD (A:51%, B: 27%, P=0.56, Table 4). In 43% of the study population, the proximal entry diameter was >10mm, measured and calculated in 3-dimensional multiplanar reformats. (A: 26%, B: 18%; P=0.22, Table 4) (Mustafi et al., 2020).

TABLE 3: Baseline patients and dissection characteristics (Mustafi et al., 2020)

	Overall n=74	Conservative n=50	Acute TEVAR n=24	p-values
Age (years)	62 (±2)	62 (±2)	62 (±5)	0.9888
Female gender	21 (28%)	17 (23%)	4 (5%)	0.1704
Treated with TEVAR	42 (57%)	18 (36%)	24 (100%)	<0.0001
Follow-up after TEVAR (days)	491 (±88)	509 (±145)	477 (±110)	0.8335
Time to TEVAR after dissection (days)	558 (±180)	1298 (±355)	4 (±1)	<0.0001
Total follow-up (days)	1278 (±158)	1625 (±209)	554 (±129)	0.001

Ordinal data are n (%).

Continuous data are mean ± standard error.

TEVAR thoracic endovascular aneurysm repair.

TABLE 4: Anatomic risk factors for aortic enlargement (Mustafi et al., 2020)

	Overall n=74	Conservative n=50	Acute TEVAR n=24	p-values
Entry tear at inner curvature	17 (23%)	8 (11%)	9 (12%)	0.0738
Partial thrombosis of the false lumen before TEVAR	26 (35%)	15 (20%)	11 (15%)	0.2027
Entry diameter>10 mm	32 (43%)	19 (26%)	13 (18%)	0.2174
Entry diameter >20 mm	15 (20%)	10 (14%)	5 (6%)	0.9335
Baseline false lumen diameter >22 mm	58 (78%)	38 (51%)	20 (27%)	0.5584
Baseline aortic diameter >40 mm	43 (58%)	31 (42%)	12 (16%)	0.4507

Ordinal data are n (%).

Continuous data are mean ± standard error.

TEVAR thoracic endovascular aneurysm repair.

3.2 Procedural data and the follow-up

TEVAR was implanted through a transfemoral approach with the use of rapid pacing in all patients. The procedural details of the endovascular procedure are provided in Table 5.

The mean stent graft length was 176±5 mm (Table 5). In 71% (n=30) of patients, the TEVAR procedure was performed in landing zone II and in 29% (n=12) of patients in landing zone III. In 97% of patients with TEVAR in the landing zone II the revascularization of the left subclavian artery was successfully implemented (Table 5) (Mustafi et al., 2020).

In the follow-up period, one patient from the conservative group was diagnosed with an aneurysm of the ascending aorta and two patients from the same group developed Stanford TAAD. All three patients required open aortic surgery (Mustafi et al., 2020).

During the follow-up, total mortality was 18%, most notable in group A with 20% (n=10). From group B only one patient died (4%). However, there was only one case of death in our study that was related directly to the aorta and that was one patient from the conservative treatment group, who died of aortic rupture (Mustafi et al., 2020).

TABLE 5: Periprocedural data (Mustafi et al., 2020)

Periprocedural characteristics	Overall n=42
Landing zone II	30 (71)
LSA revascularization (TEVAR zone II)	29 (97)
Landing zone III	12 (29)
Transfemoral approach	42 (100)
Mean stent graft length (mm)	176 ± 5
Rapid pacing	42 (100)
Primary entry covered	42 (100)

Continuous data are mean ± standard error and ordinal data are *n* (%)

TEVAR thoracic endovascular aortic repair

LSA left subclavian artery

3.3 Aortic diameter growth rates

Regarding group A (n=50) and group B (n=24), our analysis showed a significant difference in growth rate at the D5 segment (mid-descending aorta). Group A showed the aortic diameter growth at D5 (+7 mm/year) and group B at the same segment shrinkage of -4 mm/year (D5: A: +7±3 mm/year; B: -4+-3 mm/year; P=0.003; Table 6). The patients treated with TEVAR in the acute phase showed

unsignificant shrinkage in the mid-ascending aorta (D1: -0±2 mm/year; P=0.80), the distal ascending aorta (D2: -3±2 mm/year; P=0.99), the mid-arch (D3: -2±3 mm/year; P=0.67) and the proximal descending aorta (D4: -2±3 mm/year; P=0.10, Table 6). Group B showed a significant increase of distal descending diameter at the coeliac trunk, whereas a reduction at the same landmark was seen in group A (D6: A: -2±2 mm/year; B: +7±3 mm/year; P=0.023; Table 6) (Mustafi et al., 2020).

The analysis of two subgroups of group A showed remarkable differences in growth rates. In non-converted patients unchanged diameters or reduction was seen in the mid-arch (D3: 0±2 mm/year; P=0.015), the proximal descending aorta (D4: -3±2 mm/year; P<0.001), the mid-descending aorta (D5: 0±1 mm/year; P<0.001), the distal descending aorta at the coeliac trunk (D6: -4±2 mm/year; P=0.003) and in the mid-abdominal aorta (D7: -3±2 mm/year; P=0.04; Table 7). In the subgroup of patients before conversion the aortic diameters increased significantly (D3: +2±2 mm/year, P=0.03; D4: +10±4mm/year P<0.001; D5: +18±7 mm/year, P<0.001; D6: +2±2 mm/year, P=0.049 and D7: +3±2 mm/year, P=0.007; Table 7). Both subgroups showed decrease of diameter in mid-ascending and distal ascending aorta (D1: non-converted: -3±2 mm/year; converted: -1±1 mm/year; P=0.16; D2: non-converted: -2±1 mm/year; converted: -1±1 mm/year; P=0.29; Table 7) (Mustafi et al., 2020). These changes were unsignificant.

The observed risk factors of aortic diameter enlargement in the non-converted (n=32) and converted (n=18) chronic dissection subgroups are shown in Table 8. Baseline aortic diameter >40 mm was seen in CT scans in 78% (n=14) of patients with conversion and in 53% (n=17) of conservatively-treated patients (P=0.13) without conversion to TEVAR. In 94% (n=17) of converted and in 66% (n=21) of non-converted patients the baseline false lumen diameter >22 mm (P=0.036, Table 8) was noticed. Generally, all evaluated risk factors had a higher incidence in the subgroup of patients converted to TEVAR, with exception of partial thrombosis of the false lumen in baseline CT scan (non-converted: 34%, n=11; converted: 22%, n=4; P=0.52, Table 8) (Mustafi et al., 2020).

Table 9. presents the diameter changes within the converted subgroup before and after the conversion to TEVAR. Significant growth in the proximal descending and mid-descending aorta was measured before the conversion (D4: +11±4 mm/year; D5: +18±7 mm/year; P<0.001, Table 9). After the conversion in follow-up CT scans the reduction of diameter at the same landmarks (D4: -9±4 mm/year; D5: -14±3 mm7year; P<0.001, Table 9) was noticed. The diameter shrinkage in the distal ascending aorta before the conversion (D2 -1±1 mm/year) turned to aortic diameter growth after the TEVAR procedure (D2: +2±4 mm/year; P=0.77, Table 9) although those observations were not considered relevant (Mustafi et al., 2020).

TABLE 6: Axial aortic diameter growth rate (mm/year) in dissections after conservative therapy and TEVAR in the acute phase (Mustafi et al., 2020)

Aortic diameter landmarks	Conservative n=50	Acute TEVAR n=24	p-values
D1	-2.68 (+/-1.11)	-0.04 (+/-1.93)	0.8039
D2	-1.52 (+/-0.65)	-2.93 (+/-2.20)	0.9954
D3	0.87 (+/-1.34)	-2.00 (+/-2.95)	0.6734
D4	2.01 (+/-1.92)	-1.88 (+/-2.68)	0.1023
D5	6.67 (+/-2.87)	-4.27 (+/-2.53)	0.0033
D6	-2.17 (+/-1.72)	7.07 (+/-2.84)	0.0233
D7	-0.52 (+/-1.51)	2.81 (+/-1.42)	0.3897

Data are mean growth rates ± standard error mm/year.

TEVAR thoracic endovascular aneurysm repair.

D1 Mid-ascending diameter.

D2 Distal ascending diameter at the brachiocephalic trunk.

D3 Mid-arch diameter.

D4 Proximal descending diameter.

D5 Mid-descending diameter.

D6 Distal descending diameter at the celiac trunk.

D7 Mid-abdominal diameter.

TABLE 7: Axial aortic diameter growth rate (mm/year) in non-converted and converted chronic dissections before conversion to TEVAR (Mustafi et al., 2020)

Aortic diameter landmark	Non-converted n=32	Converted n=18	p-values
D1	-3.36 (+/-1.56)	-1.46 (+/-1.34)	0,1601
D2	-1.96 (+/-0.68)	-0.72 (+/-1.34)	0.2886
D3	0.20 (+/-1.84)	2.07 (+/-1.80)	0,0145
D4	-2.84 (+/-1.73)	10.62 (+/-3.61)	<0.0001
D5	0.40 (+/-1.29)	17.82 (+/-7.02)	<0.0001
D6	-4.37 (+/-2.41)	1.75 (+/-1.86)	0.0027
D7	-2.61 (+/-2.02)	3.21 (+/-1.91)	0.0402

Data are mean growth rates ± standard error mm/year.

D1 Mid-ascending diameter.

D2 Distal ascending diameter at the brachiocephalic trunk.

D3 Mid-arch diameter.

D4 Proximal descending diameter.

D5 Mid-descending diameter.

D6 Distal descending diameter at the celiac trunk.

D7 Mid-abdominal diameter.

TABLE 8: Anatomic risk factors for aortic enlargement in the non-converted and converted chronic dissection subgroup (Mustafi et al., 2020)

	Non-converted n=32	Converted n=18	p-values
Entry tear at inner curvature	4 (13%)	4 (22%)	0.4357
Partial thrombosis of the false lumen before TEVAR	11 (34%)	4 (22%)	0.5231
Entry diameter>10 mm	11 (34%)	8 (44%)	0.5516
Entry diameter >20 mm	6 (19%)	4 (22%)	1.0000
Baseline false lumen diameter >22 mm	21 (66%)	17 (94%)	0.0361
Baseline aortic diameter >40 mm	17 (53%)	14 (78%)	0.1299

Ordinal data are n (%).

Continuous data are mean ± standard error.

TEVAR thoracic endovascular aneurysm repair.

TABLE 9: Axial aortic growth rate (mm/year) in chronic dissection before and after conversion to TEVAR (Mustafi et al., 2020)

Aortic diameter landmarks	Before conversion n=18	After conversion n=18	p-values
D1	-1.46 (+/-1.34)	-0.40 (+/-1.63)	0.7337
D2	-0.72 (+/-1.34)	1.79 (+/-3.61)	0.7660
D3	2.07 (+/-1.80)	1.82 (+/-2.22)	0.7019
D4	10.62 (+/-3.61)	-9.48 (+/-3.75)	0.0001
D5	17.82 (+/-7.02)	-14.22 (+/-3.09)	<0.0001
D6	1.75 (+/-1.86)	6.27 (+/-3.32)	0.4171
D7	3.21 (+/-1.91)	8.10 (+/-7.48)	0.1815

Data are mean growth rates ± standard error mm/year.

D1 Mid-ascending diameter.

D2 Distal ascending diameter at the brachiocephalic trunk.

D3 Mid-arch diameter.

D4 Proximal descending diameter.

D5 Mid-descending diameter.

D6 Distal descending diameter at the celiac trunk.

D7 Mid-abdominal diameter.

3.4 Aortic length growth rates

The aortic length measurements were divided into four segments: L1 (ascending aorta), L2 (aortic arch), L3 (descending aorta), and L4 (abdominal aorta). Table 10 gives an overview of the comparison in aortic length changes between the two study groups. Both groups showed stable lengths or even shortening in the ascending aorta (L1: A: 0±1 mm/year, B: 0±0 mm/year, P=0.53) and the aortic arch (L2: A: 0±0 mm/year, B: 0±0 mm/year, P=0.70; Table 10). In group A the unsignificant enlargement in the descending aorta was present (L3: +3±3 mm/year, P=0.88), which correlates with diameter growth in the same segment (D4: +2±2 mm/year, D5: +7±3 mm/year, Table 10). At the same landmark in group B a slight increase in length (L3: 0±1 mm/year, P=0.88, Table 10) was observed. In the abdominal aorta, no correlation between diameter and length changes for group A (D7: -1±2 mm/year, P=0.39; L4: +2±2 mm/year, P=0.009) as well as for group B (D7: +3±1 mm/year, P=0.39; L4: 0±0 mm/year, P=0.009, Table 10) could be detected (Mustafi et al., 2020).

The analysis of the subgroups showed the elongation in “non-converted” patients in the ascending aorta (L1: +1±2 mm/year, P=0.17), the descending aorta (L3: 5±5 mm/year, P=0.049) and in the abdominal aorta (L4: +1±2 mm/year, P=0.86) with exception of the aortic arch, where shortening was noticed (L2: 0±0 mm/year, P=0.40, Table 11). There was no correlation to diameter changes in corresponding landmarks. In the group of “converted” patients before the conversion, all aortic length segments were regressive except the abdominal aorta (L4: +3±2 mm/year, P=0.86, Table 11) (Mustafi et al., 2020).

Comparing the patients before and after conversion we noticed that the elongation in the abdominal aorta (L4: +3±2 mm/year) turned to shortening (L4: -3±3 mm/year, P=0.61, Table 12) after TEVAR. However, the corresponding diameter rates were steadily increasing, independent of the endovascular procedure (D6: before: +2±2 mm/year, after: +6±3 mm/year, P=0.42; D7: before: +3±2 mm/year, after: +8±7 mm/year, P=0.18; Table 12). However, the patients experienced length regression in ascending aorta before the conversion (L1: -

1±1 mm/year), which turned into elongation (L1: +2±2 mm/year, P=0.37, Table 12) after the treatment (Mustafi et al., 2020).

TABLE 10: Longitudinal aortic growth rate (mm/year) in dissections after conservative therapy and TEVAR in the acute phase (Mustafi et al., 2020)

Aortic segment lengths	Conservative n=50	Acute TEVAR n=24	p-values
L1	0.49 (+/-1.10)	0.22 (+/-0.31)	0.5291
L2	-0.44 (+/-0.29)	-0.11 (+/-0.12)	0.6989
L3	3.22 (+/-3.20)	0.23 (+/-0.76)	0.8761
L4	2.06 (+/-1.58)	-0.06 (+/-0.32)	0.0089

Data are mean growth rates ± standard error (mm/year).

TEVAR thoracic endovascular aneurysm repair.

L1 Ascending aorta length.

L2 Aortic arch length.

L3 Descending aorta length.

L4 Abdominal aorta length.

TABLE 11: Longitudinal aortic growth rate (mm/year) in non-converted and converted chronic dissections before conversion to TEVAR (Mustafi et al., 2020)

Aortic segment lengths	Non-converted n=32	Converted n=18	p-values
L1	1.43 (+/-1.65)	-1.18 (+/-0.82)	0.1662
L2	-0.19 (+/-0.36)	-0.87 (+/-0.49)	0.4016
L3	5.35 (+/-4.89)	-0.57 (+/-1.81)	0.0488
L4	1.48 (+/-2.15)	3.10 (+/-2.24)	0.8636

Data are mean growth rates ± standard error (mm/year).

L1 Ascending aorta length.

L2 Aortic arch length.

L3 Descending aorta length.

L4 Abdominal aorta length.

TABLE 12: Longitudinal aortic growth rate (mm/year) in chronic dissection before and after conversion to TEVAR (Mustafi et al., 2020)

Aortic segment lengths	Before conversion n=18	After conversion n=18	p-values
L1	-1.18 (+/-0.82)	1.94 (+/-1.87)	0.3692
L2	-0.87 (+/-0.49)	-0.95 (+/-0.50)	0.7337
L3	-0.57 (+/-1.81)	-2.12 (+/-1.10)	0.0237
L4	3.25 (+/-2.24)	-2.92 (+/-3.31)	0.6095

Data are mean growth rates ± standard error (mm/year).

L1 Ascending aorta length.

L2 Aortic arch length.

L3 Descending aorta length.

L4 Abdominal aorta length.

4 Discussion

4.1 Remodelling of aortic dissections

Remodeling in aortic dissection starts after covering the primary entry tear with TEVAR and the induction of the thrombosis of the false lumen which is related to a higher aorta-related survival in the midterm. The persistence of false lumen perfusion leads to the progression of the dissection (Yang et al., 2012, Mani et al., 2012, Andacheh et al., 2012).

The systematic review by Patterson *et al.* which included 16 different studies showed that the TEVAR procedure for acute aortic dissection led to a a significant reduction of false lumen diameters and to the significant expansion of true lumen. The process continued for up to 5 years (Patterson et al., 2014). In the group of patients with chronic TBAD treated with TEVAR the changes were more variable, and complete false lumen thrombosis occurred in 38% to 91.3% of cases. It is assumed that the aorta is less suitable for remodeling in the cronic phase due to the thicker septum with multiple fenestrations (Yang et al., 2012). However, recent studies favor remodeling in both acute and chronic phases. Chou *et al.* found no significant difference in the true lumen expansion or false lumen regression between acute and chronic groups during the follow-up (Chou et al., 2018). Lescan *et al.* showed a comparable effect of TEVAR in both phases as well (Lescan et al., 2019).

The reason for the variable rate of aortic remodeling in chronic dissections might be diverse perioperative practices between different centers (Patterson et al., 2014). Qing *et al.* found a more favorable remodeling at an average follow-up of 36 months in patients with a longer stent graft (>162 mm) (Qing et al., 2012). A longer aortic coverage may result in a mechanical compression of the false lumen and more downstream reentry tears may be covered (Patterson et al., 2014). Andacheh *et al.* reported that the TBAD extending below the renal arteries was less likely to result in favorable aortic remodeling after TEVAR, probably because in these cases covering the aortic segment with stent graft above the diaphragm will often not include the main reentry tear below the diaphragm (Andacheh et al., 2012).

Brunkwall *et al.* and Nienaber *et al.* evaluated the aortic remodeling in their randomized trials (Brunkwall et al., 2014, Nienaber et al., 2009). The first author showed a favorable effect of endovascular repair on aortic remodeling compared with patients treated conservatively in the acute setting. The second author observed improved aortic remodeling after 2 years in patients with uncomplicated TBAD treated with TEVAR in the subacute phase.

The change of the aortic diameter is a recognized method to rate aortic remodeling (Matsuda et al., 2010). We compared remodeling after conservative treatment and TEVAR calculating the mean growth rates of the aortic diameters. The group of patients treated with TEVAR in the acute phase experienced a higher shrinkage of the aortic diameters in proximal descending and mid-descending aortic segment than group A treated conservatively. Observing the two subgroups, the strongest remodeling was noticed in the conservative group after conversion to TEVAR in the chronic phase (Mustafi et al., 2020).

In the retrospective cohort study by Chou *et al.,* no aortic remodeling was noticed in the distal abdominal aorta. Covering only the proximal primary tear leaves the distal re-entries uncovered which leads to persistent flow in the aortic segment below the coeliac trunk (Chou et al., 2018). In this context, Wojciechowski *et al.* reported stable diameters at the coeliac trunk and abdominal levels as well as shrinkage of aortic diameter in the mid-descending aorta (Wojciechowski et al., 2019). In our study, after TEVAR both acute and chronic groups of patients showed diameter growth at the distal descending aorta at the coeliac trunk (D6) as well at the mid-abdominal diameter level (D7). It might be the result of our treatment regime, which includes covering only the proximal entry tear, leaving the downstream re-entries uncovered (Mustafi et al., 2020). The extensive aortic coverage increases the risk of neurological complications. Matsuda *et al.* observed in their study a significantly higher incidence of paraplegia in patients with longer operation time and longer stent grafts (Matsuda et al., 2010).

4.2 Conversion from conservative therapy to thoracic endovascular aortic repair

Aneurysmal dilatation is one of the late complications in patients with TBAD treated conservatively, leading to aortic growth in follow-up CT scans (Song et al., 2007). The aortic diameter growth rate in patients with conservatively treated TBAD was addressed in several studies. Sueyoshi *et al.* reported diameter growth in one or more aortic segments in 84% of patients. The only significant risk factor for the increase in this study was the presence of blood flow in the false lumen (Sueyoshi et al., 2004). For non-operated patients, aortic widening is mostly the result of false lumen expansion (Kelly et al., 2007). Onitsuka *et al.* identified a maximum aortic diameter >40 mm in baseline CT scans and patent false lumen as the predictive factors of aortic diameter growth in follow-up (Onitsuka et al., 2004). However, these studies were based on monitoring patients with CT scans at least one year apart, excluding the possibility of rapid aortic expansion in the first year. Including those groups of patients, Durham *et al.* observed a greater rate of total aortic enlargement than in the studies mentioned above, and as a predictor of aortic enlargement featured an initial aortic diameter >35 mm (Durham et al., 2015).

In almost two-thirds of patients with chronic TBAD, conservative therapy results in stagnation of aortic diameter growth. Although, there are a few risk factors that lead to false lumen expansion and consequently conversion to endovascular treatment. The risk factors of aortic growth in uncomplicated TBAD were observed by Bogerijen *et al.* in a meta-analysis that reviewed a total of 18 articles covering that topic (van Bogerijen et al., 2014). Nearly half of those studies have shown that a maximum aortic diameter >40 mm correlates with aortic growth (van Bogerijen et al., 2014). Furthermore, multiple studies showed complete thrombosis of the false lumen to be a protective factor against future aortic enlargement. However, most of these studies estimated the patency of the false lumen based on the CT scan right after the index event (van Bogerijen et al., 2014). In the initial CT scans after dissection onset, the false lumina are mostly patent (Sueyoshi et al., 2004). Therefore, it is important to proceed with the CT

scan before the discharge to evaluate false lumen patency after enabling aortic remodeling with appropriate anti-hypertensive therapy (Durham et al., 2015).
In our study, the conversion from conservative to endovascular treatment was 36% (n=18). As the significant risk factor for aortic enlargement, the false lumen diameter >22 mm was present in 94% of converted patients and 66% of non-converted and baseline aortic diameter >40 mm in 78% of converted and 53% of non-converted patients (Mustafi et al., 2020). Song *et al.* found the false lumen diameter to be the most powerful predictor of late aneurysmal change. This study also showed that the initial false lumen diameter correlates better than the initial aortic diameter with the rate of aortic dilatation in the follow-up. They observed the false lumen diameter >22 mm in initial CT scans to be the independent risk factor for future aortic enlargement. The high false lumen perfusion pressure may be the major trigger for further dilatation of the false lumen and generally for the aortic expansion (Song et al., 2007).

4.3 Aortic elongation

At this point, the longitudinal change in aortic length, particularly regarding the remodeling after aortic dissection has been poorly investigated (Mustafi et al., 2020). Chen *et al.* observed the aortic elongation after TEVAR in a retrospective study that included patients who had a follow-up CT scan in each of the five years after the procedure. They spotted a length growth rate of 1.7 mm/year in the aortic segment between the brachiocephalic trunk and coeliac trunk, with the most pronounced changes in the aortic arch (Chen et al., 2020). Spinella *et al.* compared the changes in aortic length in the first year and the first month follow-up CT scans after hybrid TEVAR. The results showed significant elongation in the first year from the aortic root to the proximal edge of the left subclavian artery. However, the length changes in the descending aorta, from the left subclavian artery to the distal landing zone, were not statistically significant (Spinella et al., 2019). Regarding the elongation after endovascular aortic aneurysm repair (EVAR), Chandra *et al.* described significant lengthening in the multiple aortoiliac

segments, but not in the iliofemoral segments in a period of three years after the procedure (Chandra et al., 2015).

Michineau *et al.* observed length changes in the aorta depending on diameter growth using the aortic xenograft model of abdominal aortic aneurysm in rats and spotted a positive correlation between these two parameters (Michineau et al., 2010). Aortic morphology is associated with age as well. Boufi *et al.* showed in a study of 123 patients without thoracic aorta pathology the posterior arch lengthening and the aortic diameter extension (Boufi et al., 2017). In another study, Sugawara *et al.* found that the ascending aorta length increased significantly with aging even without the presence of cardiovascular disease, whereas the descending aorta was not affected by this process. The authors assumed that the reason for such dynamics may be the anatomical position of the proximal aorta, which absorbs left ventricular ejection and local pulsatile pressure (Sugawara et al., 2008). However, a recent cross-sectional single-center study by Adriaans *et al.* describes the most pronounced length changes in the proximal descending aorta caused by aging (Adriaans et al., 2018).

Aortic elongation might be not just a consequence of aortic dissection, but also an independent risk factor for its occurrence. Lescan *et al.* found the aortic arch length to be enlarged in patients with TBAD in CT scans before this event, while Krüger *et al.* described similar changes preceding the TAAD (Lescan et al., 2017, Kruger et al., 2018).

To compare whether the aortic elongation depends on diameter changes and to evaluate the impact of remodeling on lengthening, we included the length growth rate in our measurements. The aortic length changes were negligible at all segments (range 0 to 3 mm/year; max. relative length growth 1%) compared to the diameter growth changes (range -4 to 7 mm/year; max. relative diameter growth +18%). Those discrete changes unable the use the aortic length change as the remodeling marker (Mustafi et al., 2020).

In our study, the group of patients treated acutely with TEVAR experienced shortening or stagnation of the abdominal aorta (L4: -0.06±0.32 mm/year; P=0.009). The comparison of the subgroup lengths before and after conversion showed that the elongation rate in the abdominal aorta of +3.25±2.24 mm/year

turned to aortic length reduction of -2.92±3.31 mm/year (L4; P=0.61, Table 12) after TEVAR.

In group A the elongation of descending aorta correlated positively with the diameter growth in the mid-descending aorta (D5: 6.67±2.87 mm/year and L3: 3.22±3.20 mm/year; R=0.38; P=0.007). In group B no correlation was noticed at the same landmarks (D5: -4.27±2.53 mm/year and L3: 0.23±0.76 mm/year; R=0.32; P=0.13). This might be the result of uneven distribution of remodeling in the descending aorta due to diameter reduction with stent graft treated and diameter increase in distal non-treated aortic segment. However, our study detected no correlation between diameter and length changes in the descending aorta (Mustafi et al., 2020).

Our study has potential limitations. To evaluate aortic remodeling in conservative and endovascular-treated TBAD we created a retrospective single-center study. The number of subjects included in this research and the power of the study are low. To address this problem and to confirm our results, a prospective multicenter approach with 3 treatment groups of patients (conservative treatment and TEVAR in acute and chronic phases) is required (Mustafi et al., 2020).

5 Conclusions

To compare aortic remodeling in conservative and endovascular-treated patients after TBAD, we divided the aorta into several segments and observed the diameter and length changes in both groups of patients. Additionally, we observed the correlation between the dynamics of these two parameters. In comparison to the diameter changes, the aortic length changes in our study were subtle in all segments.

In the conservative group, a positive correlation between the length of the descending aorta and the diameter expansion in the mid-descending aorta was noticed. However, no correlation at the same landmarks was present after TEVAR in the acute phase (group B). Therefore, those discrete length changes do not correlate consistently with the aortic diameter changes (Mustafi et al., 2020).

In acute TBAD a certain irregularity in remodeling distribution after TEVAR was noticed. The diameter shrinkage was present in the covered proximal part of the aorta. In the distal uncovered part, the expansion of the aortic diameter after endovascular treatment was more pronounced than after conservative treatment. After conversion in the chronic phase, TEVAR induced the strongest remodeling in the proximal descending and mid-descending part of the aorta, which was more pronounced than in the acute phase.

Regarding the length changes, in the conservatively treated group, we spotted an elongation in the descending and the abdominal aorta. In group B TEVAR procedure slowed down this process and the elongation was less pronounced at the same landmarks. In the converted group of patients, TEVAR prevented further elongation and led to shortening in the evaluated segments (Mustafi et al., 2020).

Following risk factors favoring the diameter enlargement during the follow-up in uncomplicated TBAD were also evaluated: primary entry diameter >10 mm, primary entry diameter >20 mm, baseline aortic diameter >40 mm, baseline false lumen diameter >22 mm, entry at the smaller aortic arch curvature, and partial thrombosis of the false lumen. All the risk factors except partial false lumen thrombosis were mainly seen in the converted subgroup of patients. The false

lumen diameter >22mm proved to be the major risk factor for aortic dilatation and was found in 94% of converted patients in the baseline CT scans (Mustafi et al., 2020).

Regular follow-up CT scans are necessary to identify patients with high growth rates under conservative treatment and to set an indication for TEVAR procedure promptly in the chronic phase. Our research was designed as a single-center retrospective study with a low number of patients included in the analysis. Therefore, further prospective multicenter studies with more subjects are indispensable to confirm our findings, verify the clinical value of our results and allow a more sophisticated analysis of the dynamic of aortic morphology. Thus, by recognizing proven factors for aortic enlargement, high-risk patients could be earlier converted to TEVAR (Mustafi et al., 2020).

6 Summary

6.1 Summary (English version)

The patients with diagnosed TBAD are initially treated with antihypertensive agents, reducing the heart rate and systolic blood pressure (Isselbacher, 2005). While the therapy of the non-complicated TBAD remains conservative to the chronic phase, the complicated TBADs are treated with TEVAR to prevent further extension and diameter progression, malperfusion, and aortic rupture in the acute phase (Onitsuka et al., 2004). The signs and symptoms which define complicated TBAD are aortic ruptures, rapid aortic expansion, malperfusion, shock, paraplegia, refractory pain, peri-aortic hematoma, and refractory hypertension (Riambau et al., 2017).

The aim of the study was to compare the aortic remodeling in the patients with TBAD treated conservatively and those treated with TEVAR in the acute phase.

All patients with TBAD admitted between 2011 and 2017 to our center with at least one CT follow-up (>6 months) were included in the current study. Group A included the conservative patients with uncomplicated TBAD, while Group B included the patients with complicated TBAD who were treated with TEVAR in the acute phase. Group A was divided into two subgroups consisting either of patients whose therapy remained conservative or those converted to TEVAR due to aortic growth in the chronic phase. The baseline CT scan and the CT of the last follow-up visit were used for three-dimensional centerline reconstruction of the aorta from the aortic valve to the 1 cm below the aortic bifurcation. Aortic diameters and aortic lengths were measured at the same anatomical landmarks in the 3D centerline reconstruction for all CT examinations (Mustafi et al., 2020).

The study included 74 patients with TBAD: 50 patients in group A and 24 patients in group B. For group A the mean duration of follow-up was 1625 ± 209 days and for group B 554 ± 129 days. The prevalence of the male gender was higher compared to the female gender (A: 77%, B: 95%; P=0.17) and the mean age in both groups was 62 years (group A 62±2; group B 62±5; P=0.99) (Mustafi et al., 2020).

In the mid-descending aorta, the aortic diameter growth rate was significantly higher in group A than in group B (A: +7 mm/year, B: -4 mm/year, P=0.003). The

group B treated with TEVAR in the acute phase showed a significant increase in diameter at the celiac trunk landmark (+7±3 mm/year; P=0.023), while the diameter remained stable in the conservatively treated group A. At all other landmarks, there was no significant difference between the groups. During the follow-up period, 18 patients (36%) from conservatively treated Group A were converted to TEVAR due to aortic diameter progression. These patients showed a significant increase in the diameter of the descending aorta of 18 mm/year (P<0.001) before conversion. The proximal and mid-descending aorta showed a reduction in growth rate after conversion to TEVAR (preoperative +11 and +18 mm/year; postoperative -9 and -14 mm/year, P<0.001) (Mustafi et al., 2020).

The study showed a significant diameter reduction after TEVAR in the acute phase in the descending aorta. However, an increase in diameter was spotted at the same landmark in the conservatively treated group. Despite the significant increase in diameter before conversion, TEVAR led to the most intensive remodeling after conversion in the chronic phase (Mustafi et al., 2020).

This study indicated that TEVAR can prevent the development of thoracic aneurysms after type B dissections. Moreover, our findings underline the importance of regular follow-up examinations in all TBAD patients to prevent future complications. Patients with a prominent diameter increase in the conservative treatment arm can be early identified and subjected to TEVAR therapy, and those with TEVAR therapy in the acute phase need to be surveilled due to the risk of aortic growth in the distal (thoracoabdominal and abdominal) aortic segments.

6.2 Summary (German version)

Alle Patienten mit diagnostizierter TBAD werden initial mit Medikamenten behandelt, die die Herzfrequenz und den systolischen Blutdruck senken (Isselbacher, 2005). Während die Therapie der unkomplizierten TBAD bis in die chronische Phase konservativ bleibt, werden die komplizierten TBADs mit TEVAR behandelt, um eine weitere Ausbreitung der Dissektion, der Zunahme

des Aortendurchmessers, oder aufgrund der Malperfusion und Aortenruptur in der akuten Phase behandelt (Onitsuka et al., 2004). Die Anzeichen und Symptome, die eine komplizierte TBAD definieren, sind Aortenruptur, rasche Aortenexpansion, Organischämie, Schock, Querschnittslähmung, refraktäre Schmerzen, periaortales Hämatom und refraktäre Hypertonie (Riambau et al., 2017).

Ziel der Studie war es, das Remodeling bei konservativ behandelten Patienten mit TBAD und der Patientengruppe die in der akuten Phase mit TEVAR behandelt wurden, zu vergleichen.

Alle Patienten mit TBAD zwischen 2011 und 2017 die an unserem Zentrum behandelt wurden mit mindestens einer CT-Nachsorgeuntersuchung (>6 Monate), wurden in die aktuelle Studie aufgenommen. Gruppe A umfasste die konservativ behandelten Patienten mit unkomplizierter TBAD, während die Gruppe B die Patienten mit komplizierter TBAD, die akut mit TEVAR behandelt wurden einschloß. Gruppe A wurde außerdem in zwei Untergruppen aufgeteilt, bestehend aus Patienten, deren Therapie konservativ blieb, und solchen, die in der chronischen Phase aufgrund des Aortenwachstums zur TEVAR Therapie konvertiert wurden. Die CT Untersuchung bei der Diagnosestellung und das CT der letzten Nachsorgeuntersuchung wurden der dreidimensionalen Centerline Rekonstruktion von der Aortenklappe bis 1 cm unterhalb der Aortenbifurkation zugeführt. Die Aortendurchmesser und Aortenlängen wurden bei allen CT-Untersuchungen an den gleichen anatomischen Orientierungspunkten in der 3D Centerline Rekonstruktion gemessen (Mustafi et al., 2020).

Die Studie schloss 74 Patienten mit TBAD ein: 50 Patienten in der Gruppe A und 24 Patienten in der Gruppe B. Für Gruppe A betrug die mittlere Dauer der Nachsorge 1625 ± 209 Tage und für Gruppe B 554 ± 129 Tage. Die Prävalenz des männlichen Geschlechtes war höher als die des weiblichen Geschlechtes (A: 77%, B: 95%; P=0.17) und das Durchschnittsalter in beiden Gruppen war 62 Jahre (Gruppe A 62±2; Gruppe B 62±5; P=0.99) (Mustafi et al., 2020).

In der mittleren Aorta descendens war die Durchmesserwachstumsrate in der Gruppe A signifikant höher als in Gruppe B (A: +7 mm/Jahr, B: -4 mm/Jahr, P=0,003). Die Gruppe, die akut mit TEVAR versorgt wurde, zeigte ein

signifikantes Wachstum des Durchmessers auf Höhe des Truncus coeliacus (+7±3 mm/Jahr; P=0.023), während der Durchmesser in der konservativ behandelten Gruppe stabil blieb. An allen anderen Messpunkten zeigte sich kein signifikanter Unterschied zwischen den Gruppen. Während des Nachsorgezeitraums wurden 18 Patienten (36 %) aus der konservativ behandelten Gruppe A aufgrund der Aortendiameterprogredienz zur TEVAR Therapie konvertiert. Diese Patienten zeigten vor der Konversion eine signifikante Zunahme des Durchmesserwachstums in der Aorta descendens von 18 mm/Jahr (P<0.001). Die proximale und mittlere Aorta descendens zeigten nach der Konversion zur TEVAR eine Verringerung der Wachstumsrate (präoperativ +11 und +18 mm/Jahr; postoperativ -9 und -14 mm/Jahr, P<0,001) (Mustafi et al., 2020).

Die Studie zeigte eine deutliche Diameterabnahme nach der TEVAR in der akuten Phase in der Aorta descendens, welche die Ausbildung thorakaler Aneurysmen durch vorbeugt (Mustafi et al., 2020). Außerdem unterstreichen unsere Ergebnisse die Bedeutung der regelmäßigen Nachsorgeuntersuchungen bei allen TBAD Patienten um künftige Komplikationen vorzubeugen. Patienten mit einer prominenten Diameterzunahme in der konservativen Therapieschiene können dadurch frühzeitig identifiziert und der TEVAR Therapie zugeführt werden. Patienten mit der TEVAR Therapie in der Akutphase benötigen eine Langzeitüberwachung aufgrund des in unserer Studie Nachgewiesenen Diameterwachstums in den distaleren (thorakoabdominellen und abdominellen) Aortensegmenten.

7 Publication

Results from this dissertation are originally published as following:

Mustafi M, Andic M, Bartos O, Grözinger G, Schlensak C, Lescan M Comparison of aortic remodelling after conservative treatment or thoracic endovascular repair in type B dissections. *Interact CardioVasc Thorac Surg 2019; doi:10.1093/icvts/ivz285*

8 References

ABURAHMA, A. F., CAMPBELL, J., STONE, P. A., NANJUNDAPPA, A., JAIN, A., DEAN, L. S., HABIB, J., KEIFFER, T. & EMMETT, M. 2009. The correlation of aortic neck length to early and late outcomes in endovascular aneurysm repair patients. *J Vasc Surg,* 50**,** 738-48.

ADACHI, H., OMOTO, R., KYO, S., MATSUMURA, M., TAMURA, F., KIMURA, S., YOKOTE, Y. & TAKAMOTO, S. 1991. [Diagnosis of acute aortic dissection with transesophageal echocardiography and results of surgical treatment]. *Nihon Kyobu Geka Gakkai Zasshi,* 39**,** 1987-94.

ADRIAANS, B. P., HEUTS, S., GERRETSEN, S., CHERIEX, E. C., VOS, R., NATOUR, E., MAESSEN, J. G., SARDARI NIA, P., CRIJNS, H., WILDBERGER, J. E. & SCHALLA, S. 2018. Aortic elongation part I: the normal aortic ageing process. *Heart,* 104**,** 1772-1777.

ALLEN, B. D., MARKL, M., BARKER, A. J., VAN OOIJ, P., CARR, J. C., MALAISRIE, S. C., MCCARTHY, P., BONOW, R. O. & KANSAL, P. 2016. Influence of beta-blocker therapy on aortic blood flow in patients with bicuspid aortic valve. *Int J Cardiovasc Imaging,* 32**,** 621-8.

ANDACHEH, I. D., DONAYRE, C., OTHMAN, F., WALOT, I., KOPCHOK, G. & WHITE, R. 2012. Patient outcomes and thoracic aortic volume and morphologic changes following thoracic endovascular aortic repair in patients with complicated chronic type B aortic dissection. *J Vasc Surg,* 56**,** 644-50; discussion 650.

BALIGA, R. R., NIENABER, C. A., BOSSONE, E., OH, J. K., ISSELBACHER, E. M., SECHTEM, U., FATTORI, R., RAMAN, S. V. & EAGLE, K. A. 2014. The role of imaging in aortic dissection and related syndromes. *JACC Cardiovasc Imaging,* 7**,** 406-24.

BARTOS, O., MUSTAFI, M., ANDIC, M., GROZINGER, G., ARTZNER, C., SCHLENSAK, C. & LESCAN, M. 2020. Carotid-axillary bypass as an alternative revascularization method for zone II thoracic endovascular aortic repair. *J Vasc Surg,* 72**,** 1229-1236.

BOUFI, M., GUIVIER-CURIEN, C., LOUNDOU, A. D., DEPLANO, V., BOIRON, O., CHAUMOITRE, K., GARIBOLDI, V. & ALIMI, Y. S. 2017. Morphological Analysis of Healthy Aortic Arch. *Eur J Vasc Endovasc Surg,* 53**,** 663-670.

BRUNKWALL, J., KASPRZAK, P., VERHOEVEN, E., HEIJMEN, R., TAYLOR, P., TRIALISTS, A., ALRIC, P., CANAUD, L., JANOTTA, M., RAITHEL, D., MALINA, W., RESCH, T., ECKSTEIN, H. H., OCKERT, S., LARZON, T., CARLSSON, F., SCHUMACHER, H., CLASSEN, S., SCHAUB, P., LAMMER, J., LONN, L., CLOUGH, R. E., RAMPOLDI, V., TRIMARCHI, S., FABIANI, J. N., BOCKLER, D., KOTELIS, D., BOCKLER, D., KOTELIS, D., VON TENNG-KOBLIGK, H., MANGIALARDI, N., RONCHEY, S., DIALETTO, G. & MATOUSSEVITCH, V. 2014. Endovascular repair of acute uncomplicated aortic type B dissection promotes aortic remodelling: 1 year results of the ADSORB trial. *Eur J Vasc Endovasc Surg,* 48**,** 285-91.

BUTH, J., HARRIS, P. L., HOBO, R., VAN EPS, R., CUYPERS, P., DUIJM, L. & TIELBEEK, X. 2007. Neurologic complications associated with endovascular repair of thoracic aortic pathology: Incidence and risk factors. a study from the European Collaborators on Stent/Graft Techniques for Aortic Aneurysm Repair (EUROSTAR) registry. *J Vasc Surg,* 46**,** 1103-1110; discussion 1110-1.

CAMBRIA, R. P., BREWSTER, D. C., GERTLER, J., MONCURE, A. C., GUSBERG, R., TILSON, M. D., DARLING, R. C., HAMMOND, G., MERGERMAN, J. & ABBOTT, W. M. 1988. Vascular complications associated with spontaneous aortic dissection. *J Vasc Surg,* 7**,** 199-209.

CHANDRA, V., ROUER, M., GARG, T., FLEISCHMANN, D. & MELL, M. 2015. Aortoiliac elongation after endovascular aortic aneurysm repair. *Ann Vasc Surg,* 29**,** 891-7.

CHEN, C. K., CHOU, H. P., CHANG, Y. Y. & SHIH, C. C. 2020. Elongation of the Aorta after Thoracic Endovascular Aortic Repair: A longitudinal study. *Int J Environ Res Public Health,* 17.

CHOU, H. W., CHAN, C. Y., CHANG, C. H., LIN, C. F., CHEN, Y. S., WANG, S. S. & WU, I. H. 2018. Comparisons of aortic remodelling and outcomes after endovascular repair of acute and chronic complicated Type B aortic dissections. *Interact Cardiovasc Thorac Surg,* 27**,** 733-741.

COSELLI, J. S. 1994. Thoracoabdominal aortic aneurysms: experience with 372 patients. *J Card Surg,* 9**,** 638-47.

CRAWFORD, T. C., BEAULIEU, R. J., EHLERT, B. A., RATCHFORD, E. V. & BLACK, J. H., 3RD 2016. Malperfusion syndromes in aortic dissections. *Vasc Med,* 21**,** 264-73.

CZERNY, M., FUNOVICS, M., SODECK, G., DUMFARTH, J., SCHODER, M., JURASZEK, A., DZIODZIO, T., ZIMPFER, D., LOEWE, C., LAMMER, J., ROSENHEK, R., EHRLICH, M. & GRIMM, M. 2010. Long-term results of thoracic endovascular aortic repair in atherosclerotic aneurysms involving the descending aorta. *J Thorac Cardiovasc Surg,* 140**,** S179-84; discussion S185-S190.

DEBAKEY, M. E., HENLY, W. S., COOLEY, D. A., MORRIS, G. C., JR., CRAWFORD, E. S. & BEALL, A. C., JR. 1965. Surgical Management of Dissecting Aneurysms of the Aorta. *J Thorac Cardiovasc Surg,* 49**,** 130-49.

DUBOIS, B. G., HOUBEN, I. B., KHAJA, M. S., YANG, B., KIM, K. M., VAN HERWAARDEN, J. A., WILLIAMS, D. M. & PATEL, H. J. 2021. Thoracic Endovascular Aortic Repair in the Setting of Compromised Distal Landing Zones. *Ann Thorac Surg,* 111**,** 237-245.

DURHAM, C. A., ARANSON, N. J., ERGUL, E. A., WANG, L. J., PATEL, V. I., CAMBRIA, R. P. & CONRAD, M. F. 2015. Aneurysmal degeneration of the thoracoabdominal aorta after medical management of type B aortic dissections. *J Vasc Surg,* 62**,** 900-6.

EGGEBRECHT, H., THOMPSON, M., ROUSSEAU, H., CZERNY, M., LONN, L., MEHTA, R. H., ERBEL, R. & EUROPEAN REGISTRY ON ENDOVASCULAR AORTIC REPAIR, C. 2009. Retrograde ascending aortic dissection during or after thoracic aortic stent graft placement:

insight from the European registry on endovascular aortic repair complications. *Circulation,* 120**,** S276-81.

EPSTEIN, N. E. 2018. Cerebrospinal fluid drains reduce risk of spinal cord injury for thoracic/thoracoabdominal aneurysm surgery: A review. *Surg Neurol Int,* 9**,** 48.

ERBEL, R. 1993. Role of transesophageal echocardiography in dissection of the aorta and evaluation of degenerative aortic disease. *Cardiol Clin,* 11**,** 461-73.

ERBEL, R., BEDNARCZYK, I., POP, T., TODT, M., HENRICHS, K. J., BRUNIER, A., THELEN, M. & MEYER, J. 1990. Detection of dissection of the aortic intima and media after angioplasty of coarctation of the aorta. An angiographic, computer tomographic, and echocardiographic comparative study. *Circulation,* 81**,** 805-14.

ETZ, C. D., HOMANN, T. M., LUEHR, M., KARI, F. A., WEISZ, D. J., KLEINMAN, G., PLESTIS, K. A. & GRIEPP, R. B. 2008a. Spinal cord blood flow and ischemic injury after experimental sacrifice of thoracic and abdominal segmental arteries. *Eur J Cardiothorac Surg,* 33**,** 1030-8.

ETZ, C. D., LUEHR, M., KARI, F. A., BODIAN, C. A., SMEGO, D., PLESTIS, K. A. & GRIEPP, R. B. 2008b. Paraplegia after extensive thoracic and thoracoabdominal aortic aneurysm repair: does critical spinal cord ischemia occur postoperatively? *J Thorac Cardiovasc Surg,* 135**,** 324-30.

ETZ, C. D., PLESTIS, K. A., KARI, F. A., LUEHR, M., BODIAN, C. A., SPIELVOGEL, D. & GRIEPP, R. B. 2008c. Staged repair of thoracic and thoracoabdominal aortic aneurysms using the elephant trunk technique: a consecutive series of 215 first stage and 120 complete repairs. *Eur J Cardiothorac Surg,* 34**,** 605-14; discussion 614-5.

EVANGELISTA, A., FLACHSKAMPF, F. A., ERBEL, R., ANTONINI-CANTERIN, F., VLACHOPOULOS, C., ROCCHI, G., SICARI, R., NIHOYANNOPOULOS, P., ZAMORANO, J., EUROPEAN ASSOCIATION OF, E., DOCUMENT, R., PEPI, M., BREITHARDT, O. A. & PLONSKA-GOSCINIAK, E. 2010. Echocardiography in aortic diseases: EAE recommendations for clinical practice. *Eur J Echocardiogr,* 11**,** 645-58.

EVANGELISTA, A., ISSELBACHER, E. M., BOSSONE, E., GLEASON, T. G., EUSANIO, M. D., SECHTEM, U., EHRLICH, M. P., TRIMARCHI, S., BRAVERMAN, A. C., MYRMEL, T., HARRIS, K. M., HUTCHINSON, S., O'GARA, P., SUZUKI, T., NIENABER, C. A., EAGLE, K. A. & INVESTIGATORS, I. 2018. Insights From the International Registry of Acute Aortic Dissection: A 20-Year Experience of Collaborative Clinical Research. *Circulation,* 137**,** 1846-1860.

FRUEHWALD, F. X., NEUHOLD, A., FEZOULIDIS, J., GLOBITS, S., MAYR, H., WICKE, K. & GLOGAR, D. 1989. Cine-MR in dissection of the thoracic aorta. *Eur J Radiol,* 9**,** 37-41.

GENONI, M., PAUL, M., JENNI, R., GRAVES, K., SEIFERT, B. & TURINA, M. 2001. Chronic beta-blocker therapy improves outcome and reduces treatment costs in chronic type B aortic dissection. *Eur J Cardiothorac Surg,* 19**,** 606-10.

GOLDSTEIN, S. A., EVANGELISTA, A., ABBARA, S., ARAI, A., ASCH, F. M., BADANO, L. P., BOLEN, M. A., CONNOLLY, H. M., CUELLAR-

CALABRIA, H., CZERNY, M., DEVEREUX, R. B., ERBEL, R. A., FATTORI, R., ISSELBACHER, E. M., LINDSAY, J. M., MCCULLOCH, M., MICHELENA, H. I., NIENABER, C. A., OH, J. K., PEPI, M., TAYLOR, A. J., WEINSAFT, J. W., ZAMORANO, J. L., DIETZ, H., EAGLE, K., ELEFTERIADES, J., JONDEAU, G., ROUSSEAU, H. & SCHEPENS, M. 2015. Multimodality imaging of diseases of the thoracic aorta in adults: from the American Society of Echocardiography and the European Association of Cardiovascular Imaging: endorsed by the Society of Cardiovascular Computed Tomography and Society for Cardiovascular Magnetic Resonance. *J Am Soc Echocardiogr,* 28**,** 119-82.

GRANATO, J. E., DEE, P. & GIBSON, R. S. 1985. Utility of two-dimensional echocardiography in suspected ascending aortic dissection. *Am J Cardiol,* 56**,** 123-9.

GREWAL, S., CONTRELLA, B. N., SHERK, W. M., KHAJA, M. S. & WILLIAMS, D. M. 2021. Endovascular Management of Malperfusion Syndromes in Aortic Dissection. *Tech Vasc Interv Radiol,* 24**,** 100751.

HAGAN, P. G., NIENABER, C. A., ISSELBACHER, E. M., BRUCKMAN, D., KARAVITE, D. J., RUSSMAN, P. L., EVANGELISTA, A., FATTORI, R., SUZUKI, T., OH, J. K., MOORE, A. G., MALOUF, J. F., PAPE, L. A., GACA, C., SECHTEM, U., LENFERINK, S., DEUTSCH, H. J., DIEDRICHS, H., MARCOS Y ROBLES, J., LLOVET, A., GILON, D., DAS, S. K., ARMSTRONG, W. F., DEEB, G. M. & EAGLE, K. A. 2000. The International Registry of Acute Aortic Dissection (IRAD): new insights into an old disease. *JAMA,* 283**,** 897-903.

HIRATA, K., WAKE, M., KYUSHIMA, M., TAKAHASHI, T., NAKAZATO, J., MOTOTAKE, H., TENGAN, T., YASUMOTO, H., HENZAN, E., MAESHIRO, M. & ASATO, H. 2010. Electrocardiographic changes in patients with type A acute aortic dissection. Incidence, patterns and underlying mechanisms in 159 cases. *J Cardiol,* 56**,** 147-53.

ISSELBACHER, E. M. 2005. Thoracic and abdominal aortic aneurysms. *Circulation,* 111**,** 816-28.

KAJI, S. 2018. Update on the Therapeutic Strategy of Type B Aortic Dissection. *J Atheroscler Thromb,* 25**,** 203-212.

KELLY, A. M., QUINT, L. E., NAN, B., ZHENG, J., CRONIN, P., DEEB, G. M. & WILLIAMS, D. M. 2007. Aortic growth rates in chronic aortic dissection. *Clin Radiol,* 62**,** 866-75.

KHAN, I. A. & NAIR, C. K. 2002. Clinical, diagnostic, and management perspectives of aortic dissection. *Chest,* 122**,** 311-28.

KHAN, I. A., WATTANASAUWAN, N. & ANSARI, A. W. 1999. Painless aortic dissection presenting as hoarseness of voice: cardiovocal syndrome: Ortner's syndrome. *Am J Emerg Med,* 17**,** 361-3.

KRUGER, T., OIKONOMOU, A., SCHIBILSKY, D., LESCAN, M., BREGEL, K., VOHRINGER, L., SCHNEIDER, W., LAUSBERG, H., BLUMENSTOCK, G., BAMBERG, F. & SCHLENSAK, C. 2017. Aortic elongation and the risk for dissection: the Tubingen Aortic Pathoanatomy (TAIPAN) projectdagger. *Eur J Cardiothorac Surg,* 51**,** 1119-1126.

KRUGER, T., SANDOVAL BOBURG, R., LESCAN, M., OIKONOMOU, A., SCHNEIDER, W., VOHRINGER, L., LAUSBERG, H., BAMBERG, F.,

BLUMENSTOCK, G. & SCHLENSAK, C. 2018. Aortic elongation in aortic aneurysm and dissection: the Tubingen Aortic Pathoanatomy (TAIPAN) project. *Eur J Cardiothorac Surg,* 54**,** 26-33.

LEFEBVRE, V., LEDUC, J. J. & CHOTEAU, P. H. 1995. Painless ischaemic lumbosacral plexopathy and aortic dissection. *J Neurol Neurosurg Psychiatry,* 58**,** 641.

LEPAGE, M. A., QUINT, L. E., SONNAD, S. S., DEEB, G. M. & WILLIAMS, D. M. 2001. Aortic dissection: CT features that distinguish true lumen from false lumen. *AJR Am J Roentgenol,* 177**,** 207-11.

LESCAN, M., CZERNY, M., BEREZOWSKI, M., ANDIC, M., BAMBERG, F., BEYERSDORF, F., SCHLENSAK, C. & RYLSKI, B. 2019. Morphologic performance analysis of the Relay nonbare stent graft in dissected thoracic aorta. *J Vasc Surg,* 70**,** 1390-1398.

LESCAN, M., VESELI, K., OIKONOMOU, A., WALKER, T., LAUSBERG, H., BLUMENSTOCK, G., BAMBERG, F., SCHLENSAK, C. & KRUGER, T. 2017. Aortic Elongation and Stanford B Dissection: The Tubingen Aortic Pathoanatomy (TAIPAN) Project. *Eur J Vasc Endovasc Surg,* 54**,** 164-169.

LIN, J., MARROCCO, C., GALOVICH, J., KOPCHOK, G., KHOYNEZHAD, A., WALOT, I., HAJI, F., JABER, R., DONAYRE, C. & WHITE, R. 2013. Experience with early TEVAR treatment of uncomplicated type B aortic dissection. *J Cardiovasc Surg (Torino),* 54**,** 161-72.

LIU, L., ZHANG, S., LU, Q., JING, Z., ZHANG, S. & XU, B. 2016. Impact of Oversizing on the Risk of Retrograde Dissection After TEVAR for Acute and Chronic Type B Dissection. *J Endovasc Ther,* 23**,** 620-5.

MANI, K., CLOUGH, R. E., LYONS, O. T., BELL, R. E., CARRELL, T. W., ZAYED, H. A., WALTHAM, M. & TAYLOR, P. R. 2012. Predictors of outcome after endovascular repair for chronic type B dissection. *Eur J Vasc Endovasc Surg,* 43**,** 386-91.

MATSUDA, H., FUKUDA, T., IRITANI, O., NAKAZAWA, T., TANAKA, H., SASAKI, H., MINATOYA, K. & OGINO, H. 2010. Spinal cord injury is not negligible after TEVAR for lower descending aorta. *Eur J Vasc Endovasc Surg,* 39**,** 179-86.

MICHINEAU, S., DAI, J., GERVAIS, M., ZIDI, M., CLOWES, A. W., BECQUEMIN, J. P., MICHEL, J. B. & ALLAIRE, E. 2010. Aortic length changes during abdominal aortic aneurysm formation, expansion and stabilisation in a rat model. *Eur J Vasc Endovasc Surg,* 40**,** 468-74.

MOORE, A. G., EAGLE, K. A., BRUCKMAN, D., MOON, B. S., MALOUF, J. F., FATTORI, R., EVANGELISTA, A., ISSELBACHER, E. M., SUZUKI, T., NIENABER, C. A., GILON, D. & OH, J. K. 2002. Choice of computed tomography, transesophageal echocardiography, magnetic resonance imaging, and aortography in acute aortic dissection: International Registry of Acute Aortic Dissection (IRAD). *Am J Cardiol,* 89**,** 1235-8.

MUSTAFI, M., ANDIC, M., BARTOS, O., GROZINGER, G., SCHLENSAK, C. & LESCAN, M. 2020. Comparison of aortic remodelling after conservative treatment or thoracic endovascular repair in type B dissections. *Interact Cardiovasc Thorac Surg,* 30**,** 458-464.

NALLAMOTHU, B. K., MEHTA, R. H., SAINT, S., LLOVET, A., BOSSONE, E., COOPER, J. V., SECHTEM, U., ISSELBACHER, E. M., NIENABER, C.

A., EAGLE, K. A. & EVANGELISTA, A. 2002. Syncope in acute aortic dissection: diagnostic, prognostic, and clinical implications. *Am J Med,* 113**,** 468-71.

NALLAMOTHU, B. K., SAINT, S., KOLIAS, T. J. & EAGLE, K. A. 2001. Clinical problem-solving. Of nicks and time. *N Engl J Med,* 345**,** 359-63.

NAUTA, F. J., TRIMARCHI, S., KAMMAN, A. V., MOLL, F. L., VAN HERWAARDEN, J. A., PATEL, H. J., FIGUEROA, C. A., EAGLE, K. A. & FROEHLICH, J. B. 2016. Update in the management of type B aortic dissection. *Vasc Med,* 21**,** 251-63.

NEYA, K., OMOTO, R., KYO, S., KIMURA, S., YOKOTE, Y., TAKAMOTO, S. & ADACHI, H. 1992. Outcome of Stanford type B acute aortic dissection. *Circulation,* 86**,** II1-7.

NIENABER, C. A., ROUSSEAU, H., EGGEBRECHT, H., KISCHE, S., FATTORI, R., REHDERS, T. C., KUNDT, G., SCHEINERT, D., CZERNY, M., KLEINFELDT, T., ZIPFEL, B., LABROUSSE, L., INCE, H. & TRIAL, I. 2009. Randomized comparison of strategies for type B aortic dissection: the INvestigation of STEnt Grafts in Aortic Dissection (INSTEAD) trial. *Circulation,* 120**,** 2519-28.

ONITSUKA, S., AKASHI, H., TAYAMA, K., OKAZAKI, T., ISHIHARA, K., HIROMATSU, S. & AOYAGI, S. 2004. Long-term outcome and prognostic predictors of medically treated acute type B aortic dissections. *Ann Thorac Surg,* 78**,** 1268-73.

PATTERSON, B. O., COBB, R. J., KARTHIKESALINGAM, A., HOLT, P. J., HINCHLIFFE, R. J., LOFTUS, I. M. & THOMPSON, M. M. 2014. A systematic review of aortic remodeling after endovascular repair of type B aortic dissection: methods and outcomes. *Ann Thorac Surg,* 97**,** 588-95.

PRINCE, M. R., NARASIMHAM, D. L., JACOBY, W. T., WILLIAMS, D. M., CHO, K. J., MARX, M. V. & DEEB, G. M. 1996. Three-dimensional gadolinium-enhanced MR angiography of the thoracic aorta. *AJR Am J Roentgenol,* 166**,** 1387-97.

QING, K. X., YIU, W. K. & CHENG, S. W. 2012. A morphologic study of chronic type B aortic dissections and aneurysms after thoracic endovascular stent grafting. *J Vasc Surg,* 55**,** 1268-75; discussion 1275-6.

RIAMBAU, V., BOCKLER, D., BRUNKWALL, J., CAO, P., CHIESA, R., COPPI, G., CZERNY, M., FRAEDRICH, G., HAULON, S., JACOBS, M. J., LACHAT, M. L., MOLL, F. L., SETACCI, C., TAYLOR, P. R., THOMPSON, M., TRIMARCHI, S., VERHAGEN, H. J., VERHOEVEN, E. L., ESVS GUIDELINES, C., KOLH, P., DE BORST, G. J., CHAKFE, N., DEBUS, E. S., HINCHLIFFE, R. J., KAKKOS, S., KONCAR, I., LINDHOLT, J. S., VEGA DE CENIGA, M., VERMASSEN, F., VERZINI, F., DOCUMENT, R., KOLH, P., BLACK, J. H., 3RD, BUSUND, R., BJORCK, M., DAKE, M., DICK, F., EGGEBRECHT, H., EVANGELISTA, A., GRABENWOGER, M., MILNER, R., NAYLOR, A. R., RICCO, J. B., ROUSSEAU, H. & SCHMIDLI, J. 2017. Editor's Choice - Management of Descending Thoracic Aorta Diseases: Clinical Practice Guidelines of the European Society for Vascular Surgery (ESVS). *Eur J Vasc Endovasc Surg,* 53**,** 4-52.

SAKAKURA, K., KUBO, N., AKO, J., IKEDA, N., FUNAYAMA, H., HIRAHARA, T., SUGAWARA, Y., YASU, T., KAWAKAMI, M. & MOMOMURA, S. 2007.

Determinants of in-hospital death and rupture in patients with a Stanford B aortic dissection. *Circ J,* 71**,** 1521-4.
SCHEPENS, M. 2018. Type B aortic dissection: new perspectives. *J Vis Surg,* 4**,** 75.
SCHLOSSER, F. J., VERHAGEN, H. J., LIN, P. H., VERHOEVEN, E. L., VAN HERWAARDEN, J. A., MOLL, F. L. & MUHS, B. E. 2009. TEVAR following prior abdominal aortic aneurysm surgery: increased risk of neurological deficit. *J Vasc Surg,* 49**,** 308-14; discussion 314.
SHIGA, T., WAJIMA, Z., APFEL, C. C., INOUE, T. & OHE, Y. 2006. Diagnostic accuracy of transesophageal echocardiography, helical computed tomography, and magnetic resonance imaging for suspected thoracic aortic dissection: systematic review and meta-analysis. *Arch Intern Med,* 166**,** 1350-6.
SILVER, F. H., HORVATH, I. & FORAN, D. J. 2001. Viscoelasticity of the vessel wall: the role of collagen and elastic fibers. *Crit Rev Biomed Eng,* 29**,** 279-301.
SONG, J. M., KIM, S. D., KIM, J. H., KIM, M. J., KANG, D. H., SEO, J. B., LIM, T. H., LEE, J. W., SONG, M. G. & SONG, J. K. 2007. Long-term predictors of descending aorta aneurysmal change in patients with aortic dissection. *J Am Coll Cardiol,* 50**,** 799-804.
SPINELLA, G., FINOTELLO, A., CONTI, M., FAGGIANO, E., GAZZOLA, V., AURICCHIO, F., CHAKFE, N., PALOMBO, D. & PANE, B. 2019. Assessment of geometrical remodelling of the aortic arch after hybrid treatment. *Eur J Cardiothorac Surg,* 55**,** 1045-1053.
SUEYOSHI, E., SAKAMOTO, I., HAYASHI, K., YAMAGUCHI, T. & IMADA, T. 2004. Growth rate of aortic diameter in patients with type B aortic dissection during the chronic phase. *Circulation,* 110**,** II256-61.
SUGAWARA, J., HAYASHI, K., YOKOI, T. & TANAKA, H. 2008. Age-associated elongation of the ascending aorta in adults. *JACC Cardiovasc Imaging,* 1**,** 739-48.
SUZUKI, T., ISSELBACHER, E. M., NIENABER, C. A., PYERITZ, R. E., EAGLE, K. A., TSAI, T. T., COOPER, J. V., JANUZZI, J. L., JR., BRAVERMAN, A. C., MONTGOMERY, D. G., FATTORI, R., PAPE, L., HARRIS, K. M., BOOHER, A., OH, J. K., PETERSON, M., RAMANATH, V. S., FROEHLICH, J. B. & INVESTIGATORS, I. 2012. Type-selective benefits of medications in treatment of acute aortic dissection (from the International Registry of Acute Aortic Dissection [IRAD]). *Am J Cardiol,* 109**,** 122-7.
SVENSSON, L. G., CRAWFORD, E. S., HESS, K. R., COSELLI, J. S. & SAFI, H. J. 1990. Dissection of the aorta and dissecting aortic aneurysms. Improving early and long-term surgical results. *Circulation,* 82**,** IV24-38.
SYED, M. A. & FIAD, T. M. 2002. Transient paraplegia as a presenting feature of aortic dissection in a young man. *Emerg Med J,* 19**,** 174-5.
TOMIGUCHI, S., MORISHITA, S., NAKASHIMA, R., HARA, M., OYAMA, Y., KOJIMA, A. & TAKAHASHI, M. 1994. Usefulness of turbo-FLASH dynamic MR imaging of dissecting aneurysms of the thoracic aorta. *Cardiovasc Intervent Radiol,* 17**,** 17-21.

TRIMARCHI, S., NIENABER, C. A., RAMPOLDI, V., MYRMEL, T., SUZUKI, T., BOSSONE, E., TOLVA, V., DEEB, M. G., UPCHURCH, G. R., JR., COOPER, J. V., FANG, J., ISSELBACHER, E. M., SUNDT, T. M., 3RD, EAGLE, K. A. & INVESTIGATORS, I. 2006. Role and results of surgery in acute type B aortic dissection: insights from the International Registry of Acute Aortic Dissection (IRAD). *Circulation,* 114**,** I357-64.

TRIMARCHI, S., TOLENAAR, J. L., TSAI, T. T., FROEHLICH, J., PEGORER, M., UPCHURCH, G. R., FATTORI, R., SUNDT, T. M., 3RD, ISSELBACHER, E. M., NIENABER, C. A., RAMPOLDI, V. & EAGLE, K. A. 2012. Influence of clinical presentation on the outcome of acute B aortic dissection: evidences from IRAD. *J Cardiovasc Surg (Torino),* 53**,** 161-8.

VAN BOGERIJEN, G. H., TOLENAAR, J. L., RAMPOLDI, V., MOLL, F. L., VAN HERWAARDEN, J. A., JONKER, F. H., EAGLE, K. A. & TRIMARCHI, S. 2014. Predictors of aortic growth in uncomplicated type B aortic dissection. *J Vasc Surg,* 59**,** 1134-43.

VERDANT, A., COSSETTE, R., PAGE, A., BAILLOT, R., DONTIGNY, L. & PAGE, P. 1995. Aneurysms of the descending thoracic aorta: three hundred sixty-six consecutive cases resected without paraplegia. *J Vasc Surg,* 21**,** 385-90; discussion 390-1.

WILLIAMS, D. M., LEE, D. Y., HAMILTON, B. H., MARX, M. V., NARASIMHAM, D. L., KAZANJIAN, S. N., PRINCE, M. R., ANDREWS, J. C., CHO, K. J. & DEEB, G. M. 1997a. The dissected aorta: part III. Anatomy and radiologic diagnosis of branch-vessel compromise. *Radiology,* 203**,** 37-44.

WILLIAMS, D. M., LEE, D. Y., HAMILTON, B. H., MARX, M. V., NARASIMHAM, D. L., KAZANJIAN, S. N., PRINCE, M. R., ANDREWS, J. C., CHO, K. J. & DEEB, G. M. 1997b. The dissected aorta: percutaneous treatment of ischemic complications--principles and results. *J Vasc Interv Radiol,* 8**,** 605-25.

WOJCIECHOWSKI, J., ZNANIECKI, L., KASZUBOWSKI, M. & ROGOWSKI, J. 2019. Late Aortic Remodeling after Endovascular Repair of Complicated Type B Aortic Dissection-TEVAR Protects Only the Covered Segment of Thoracic Aorta. *Ann Vasc Surg,* 55**,** 148-156.

XIANG, D., KAN, X., LIANG, H., XIONG, B., LIANG, B., WANG, L. & ZHENG, C. 2021. Comparison of mid-term outcomes of endovascular repair and medical management in patients with acute uncomplicated type B aortic dissection. *J Thorac Cardiovasc Surg,* 162**,** 26-36 e1.

XIE, W., XUE, Y., LI, S., JIN, M., ZHOU, Q. & WANG, D. 2021. Left subclavian artery revascularization in thoracic endovascular aortic repair: single center's clinical experiences from 171 patients. *J Cardiothorac Surg,* 16**,** 207.

XUE, L., LUO, S., DING, H., ZHU, Y., LIU, Y., HUANG, W., LI, J., XIE, N., HE, P., FAN, X., FAN, R., NIE, Z. & LUO, J. 2018. Risk of spinal cord ischemia after thoracic endovascular aortic repair. *J Thorac Dis,* 10**,** 6088-6096.

YANG, C. P., HSU, C. P., CHEN, W. Y., CHEN, I. M., WENG, C. F., CHEN, C. K. & SHIH, C. C. 2012. Aortic remodeling after endovascular repair with stainless steel-based stent graft in acute and chronic type B aortic dissection. *J Vasc Surg,* 55**,** 1600-10.

ZEESHAN, A., WOO, E. Y., BAVARIA, J. E., FAIRMAN, R. M., DESAI, N. D., POCHETTINO, A. & SZETO, W. Y. 2010. Thoracic endovascular aortic repair for acute complicated type B aortic dissection: superiority relative to conventional open surgical and medical therapy. *J Thorac Cardiovasc Surg,* 140**,** S109-15; discussion S142-S146.

Autor Contribution

The research was performed in the Department of Thoracic, Cardiac and Vascular surgery, Tübingen University Hospital (Medizinische Univeritätsklinik Tübingen aus der Klinik für Thorax-, Herz- und Gefäßchirurgie) under the supervision of Prof. Christian Schlensak and PD Dr. med. Mario Lescan.

PD Dr. med. Mario Lescan and Mateja Andic conceived the original idea and developed the concept of this study.

The article “Comparison of aortic remodelling after conservative treatment of thoracic endovascular aortic repair in type B dissection” was written and reviewed by PD Dr. med. Mario Lescan, Dr. Migdat Mustafi and Mateja Andic, with input from all authors, listed in the publication.

The statistical analysis was performed by PD Dr. med. Mario Lescan and Mateja Andic.

All text, tables, figures and literature research in this manuscript were performed by Mateja Andic except for the following: Figure 1 is an original graphic from Medical Galery of Blausen Medical 2014, Wikijournal of Medicine, free for use and with no need for permission request.

This manuscript was proofread by PD Dr. med. Mario Lescan for coherence, accuracy and clarity.

Acknowledgments

I would like to express my deepest appreciation and gratitude to Prof. Christian Schlensak, for supporting this research project and for guiding this doctoral thesis.

I would also like to extend my gratitude to PD Dr. med. Mario Lescan for encouraging me to investigate this research topic, for his invaluable patience and support, and for providing guidance and feedback throughout this project.

I would like to thank my family for their endless support while writing this manuscript, I dedicate this work to you:
To my mother Nada and my brother Ivan who unconditionally encourage me in every goal I set for myself.
And to my father Miroslav, who is always with me. I will continue to make you proud.